HIGH TEMPERATURE SOLAR CONCENTRATORS

1 author:

Robert Pitz-Paal
German Aerospace Center (DLR)
426 PUBLICATIONS **3,242** CITATIONS

HIGH TEMPERATURE SOLAR CONCENTRATORS

Robert Pitz-Paal
Institute of Technical Thermodynamics, German Aerospace Center (DLR), Germany

Keywords: Optical concentration ratio, central receiver systems, dish/Stirling, solar furnace, selective surface, imaging / non-imaging concentrators

Contents

Summary

The use of solar energy in technical applications is often constrained due to its low energy density relative to the conventional sources of energy. Optical concentration is one option to increase the energy density of the solar radiation resulting in the possibility to use absorbers with small surfaces. Higher temperatures can be achieved under concentrated conditions, because heat losses are proportional to the absorber surface. If the final objective is to convert the solar energy into work, the thermodynamics suggests that it can be done more efficiently the higher the temperature is.

In order to understand the design of different high temperature solar concentrators, this chapter gives an comprehensive insight into the fundamentals of optical concentration systems by introducing the definition of the concentration ratio and its limits and gives examples of imaging and non-imaging systems. When analyzing the conversion of radiation energy to heat, the collector performance equation of concentrated solar high temperature systems is presented and the impact of the concentration ratio, temperature and absorber properties is discussed.

One part deals with the conversion of heat to mechanical work starting with the discussion of the Carnot cycle. As typical examples for solar high temperature applications, the Rankine cycle, the Brayton cycle and the Stirling cycle are discussed. The combination of power cycle attributes and receiver performance characteristics is presented to show the optimization potential.

In the scope of this chapter only three dimensional concentration concepts using two axis tracking are investigated, since they offer an application temperature clearly beyond 500 °C. Two axis tracking systems are dealt elsewhere. Three technical

concepts for high temperature solar concentrators are presented: dish/Stirling systems acting in the power size below 25 kW_e and central receiver systems ranging from the 10 MW to 100 MW are concepts used today mainly for high temperature power production purposes, whereas the third option, a solar furnace, is utilized as a research tool to apply very high energy densities to materials or processes under investigations. For all three options the system design and a description of different components are presented together with an analysis of the system performance and loss mechanisms. The state of the art of existing facilities is demonstrated and further development directions are pointed out.

1. Introduction

This chapter focuses on 3D two-axis tracking systems with concentration ratios higher than 500 for the generation of high temperatures beyond 500 °C. Linear one-axis tracking concentrators are presented in (*Medium Temperature Solar Concentrators (Parabolic Troughs Collectors*).

High temperature solar concentrator concepts were already known by the ancient Greeks that enlightened the Olympic fire using a burning mirror. Leonardo da Vinci proposed a technique to weld copper using concentrated solar radiation in the 15th century. In the 18th century first technical prototypes of parabolic dish concentrators were used to generate steam driving steam engines. However, when oil and natural gas became available to serve as fuels to operate engines, the interest in high temperature solar concentrators vanished due to obvious reasons. In the late 1960s and early 1970s, when it became clear that fossil fuel resources are limited and their unequal distribution lead to strong dependencies, systematic research work was started in a number of industrialized countries. Today's concepts are based on the experiences gained with a variety of prototype and research installations that were mainly erected in the 1970s and 1980s. First commercial systems were put into operation in the beginning of the 21st century.

In order to understand the technical options offered by high temperature solar concentration, Section 2 of this chapter deals extensively with the relevant fundamentals. It covers the basics of optical concentration, the conversion of radiation to heat as well as the thermodynamic cycles to convert heat to mechanical power.

In Section 3 three technical concepts of high temperature solar concentrators are presented; dish/Stirling systems and central receiver systems are applied mainly on the field of electricity production whereas solar furnaces are utilized as a research tool to apply very high energy densities to materials or processes under investigation.

2. Theoretical Background

2.1. Concentration of Radiation

Radiation energy Φ measured in W that is emitted from a source is diluted with increasing distance. This means that the energy density E measured in W m^{-2} is reduced with increasing distance, because the emitted energy is distributed over a larger

surface area. Concentration of radiation aims at increasing the energy density E of the radiant energy, in order to allow a better use of it.

A generic concentrator (see Figure 1) consists of a concentrator entrance aperture area A (in m^2) which the radiant energy enters through and an exit aperture A' from where the radiation energy leaves the concentrating system.

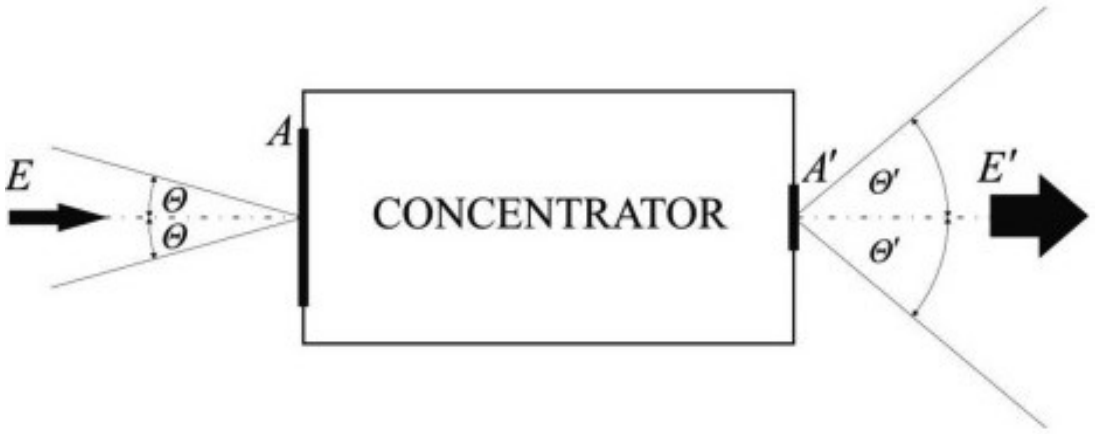

Figure 1: Scheme of a generic concentrator showing relevant aperture areas (A and A'), radiation densities (E and E') and half angles of the radiation cones (Θ and Θ')

Provided that no losses occur in the concentrator, the energy conservation principle leads to the conclusion that the concentration factor C, defined as the ratio of the outgoing energy density E' to the incoming energy density E, can also be described by the inverse ratio of the respective aperture areas:

$$C = \frac{E'}{E} = \frac{A}{A'} \qquad (1)$$

A burning glass is a simple example of a concentrator. The entrance aperture is the circular area described by the diameter of the lens, the output aperture can be arbitrarily chosen, e.g. by an orifice behind the lens, through which the radiation passes to be utilized for instance by a photovoltaic cell. An ideal lens would concentrate incoming parallel rays to a mathematical point, resulting in an infinite concentration ratio. However, in reality the focus point has finite dimensions (thus being a focal spot) so that a minimum diameter of the orifice is required to make sure that all radiation can pass. One essential reason for this is that the incoming radiation is generally not parallel but can be described by a cone with a half angle Θ. For solar energy applications on earth the sun's radiation cone with its half angle of 4.653 mrad is the relevant quantity. In complex thermodynamic considerations (cf. Welford et al., 1978) it can be shown that ideal concentrators conserve a quantity called *Etendue,* the product of aperture area and sinus square of the half angle of the radiation cone:

$$A \cdot \sin^2 \Theta = A' \cdot \sin^2 \Theta' \qquad (2)$$

Employing this law the concentration ratio of an ideal concentrator can be specified by

$$C = \frac{A}{A'} = \frac{\sin^2 \Theta'}{\sin^2 \Theta} \qquad (3)$$

For a burning glass used to concentrate the sunlight, Θ equals the sun's half angle, whereas Θ' is described by the rim rays of the lens to the focal point. For a given opening angle Θ the maximum concentration is achieved if $\sin^2\Theta' = 1$ or rather $\Theta' = 90°$. Thus, for the sun's half angle of 4.653 mrad the theoretical maximum of the concentration ratio is 46 200. From this principle the conclusion can be drawn that the concentration ratio of a burning glass is higher the smaller the ratio of focal length f to lens diameter D is, because Θ' is increased further towards 90°. However, even with a perfect burning glass the theoretical limit can not be reached. Optical errors, like the fact that parallel rays which are not parallel to the optical axis do not coincide in on single point ("off-axis aberration"), limit the capability to achieve the theoretical concentration limit.

In the analysis of concentrators it is important to distinguish between imaging and non-imaging systems. In imaging designs like the burning glass, telescopes, microscopes or parabolic shaped mirrors all rays leaving from a point of an object and entering into the aperture will be imaged on one single point in the exit aperture independently of their way through the optical systems. That is how an image can be generated. Like the example of a burning glass given above shows, inherent optical errors do not allow imaging systems (with constant refractive properties and a finite number of reflector elements) to achieve the maximum theoretical concentration ratio. For instance the simple and often applied concentrator design of an ideal 3D parabola can only reach one fourth of the theoretical limit.

Non-imaging systems only require that all rays entering the entrance aperture leave the exit aperture somewhere. It may be not surprising, that the fewer constraints of non-imaging systems lead to a higher flexibility concerning the concentrator design so that higher concentration ratios can be achieved. A simple (but sub-optimal) example is a truncated cone with reflective inner surfaces, where the radiation enters through the larger opening and leaves through the smaller one. A very efficient design of a non-imaging concentrator is a cone with a specific shape forming a segment of a parabola. Such a concentrator is called compound parabolic concentrator (CPC) (see Figure 2)**.** This design can approach the theoretical concentration limit very closely. The conservation of the *Etendue* implies that for a given ratio of exit to entrance apertures of the CPC, only rays in a cone with an half angle of

$$\Theta = \arcsin\sqrt{\frac{A'}{A}} \qquad (4)$$

will be accepted by the concentrator.

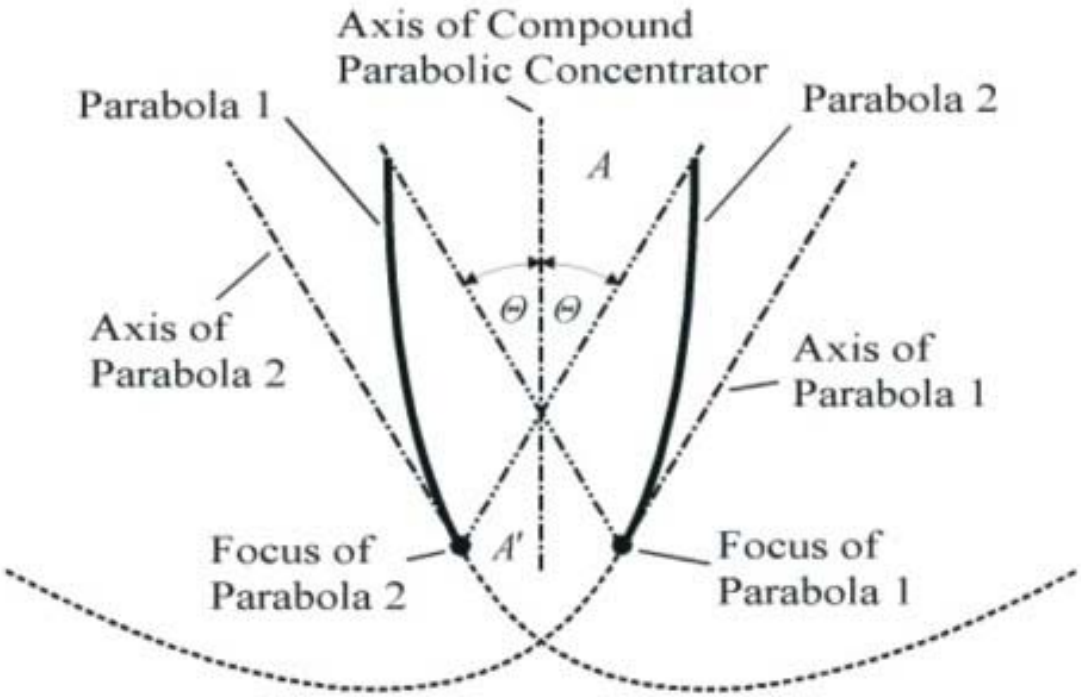

Figure 2: Compound parabolic concentrator (CPC)

A stand-alone CPC is not well suited for high temperature solar concentration, because its length needs to be very high compared to its aperture diameter to achieve high concentration ratios. However, the use of a CPC as a 3D terminal concentrator in imaging solar concentrator applications is beneficial, because it boosts the overall concentration ratio of the system by a factor of 2 to 8.

In practice, imaging mirror concentrators rather than lens concentrators are applied as primary concentrators for solar high temperature systems, due to their better outdoor durability and lower specific costs. Their design generally approximates the parabolic shape in a continuous or segmented way (see details in the subsequent paragraphs). The image of the sun if generated by such a mirror reflector is blurred by the intrinsic optical imperfections of the imaging parabola concentrator concept (off-axis aberration) and by imperfect surface characteristics. The resulting image, in particular if it consists of superimposed images of individual concentrator segments, can often be well approximated by a Gaussian distribution (see Figure 3). Thus, the energy density at the exit aperture of an imaging concentrator is not constant but varies from a peak value to zero at an infinite distance. For practical applications it makes sense to use only the central part of the Gaussian profile and to discard the rest. The amount of discarded energy is the outcome of an economic optimization process. Typical values range between 2 % and 10 %.

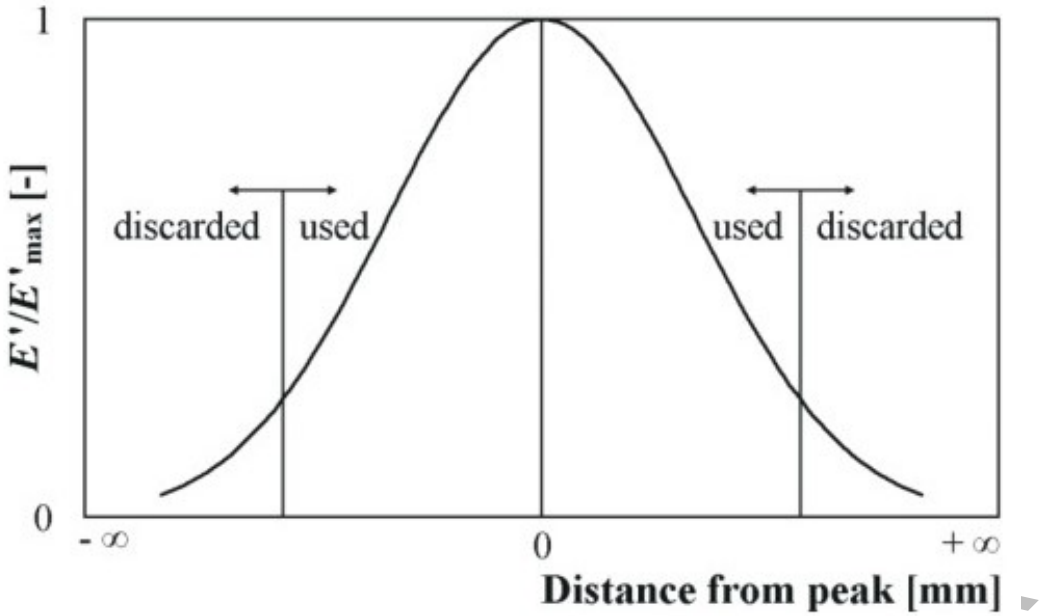

Figure 3: Gaussian distribution showing the relative radiation density (the radiation density E' related to its maximum) as a function of the distance to the center of the peak

2.2. Conversion of Radiation to Heat

The device that is used in high temperature solar concentrators for the conversion of concentrated solar radiation to heat is called "receiver". It is designed to absorb the concentrated solar radiation and to transfer as much energy as possible to a heat transfer fluid. Losses originate from the fact, that the absorbing surface may not be completely black, that it emits thermal radiation to the environment, because it has an elevated temperature, and that convection as well as conduction occur. Assuming that the receiver is not protected by a transparent cover the useful heat collected by the receiver Q can be calculated as

$$Q = A_{\mathrm{Ap}} \cdot [\alpha \cdot C \cdot E^{\mathrm{S}} - \varepsilon \cdot \sigma \cdot T_{\mathrm{A}}^4 - U_{\mathrm{L}} \cdot (T_{\mathrm{A}} - T_{\mathrm{a}})] \qquad (5)$$

with A_{Ap} being the aperture area, α being the average absorptivity of the absorber with respect to the solar spectrum, C the concentration factor, E^{S} the radiation density of the direct solar radiation and ε the average emissivity of the absorber with respect to the black body radiation at the absorber temperature T_{A}. σ stands for the Stefan-Boltzmann constant. U_{L} is the heat loss coefficient due to convection and conduction. Thermal radiation input from the ambient (with the ambient temperature T_{a}) to the receiver is neglected.

Taking into account, that for the heat transfer from the absorber to the heat transfer fluid a temperature difference is required, the following expression also holds for the useful energy:

$$Q = A_{\mathrm{Ab}} \cdot U_{\mathrm{I}} \cdot (T_{\mathrm{A}} - T_{\mathrm{F}}) \qquad (6)$$

with U_{I} being the inner heat transfer coefficient from the absorber to the fluid, T_{F} being the average temperature of the heat transfer fluid and A_{Ab} being the absorber area. Using both equations, the energy balance equation can be rewritten replacing the absorber temperature by the fluid temperature:

$$Q = A_{\mathrm{Ap}} \cdot [F \cdot \alpha \cdot C \cdot E^{\mathrm{S}} - F \cdot \varepsilon \cdot \sigma \cdot T_{\mathrm{F}}^4 - F \cdot U_{\mathrm{L}} \cdot (T_{\mathrm{F}} - T_{\mathrm{a}})] \qquad (7)$$

with the heat removal factor F, also known from the energy balance of flat plate collectors, that is defined as

$$F = \frac{A_{\mathrm{Ab}} \cdot U_{\mathrm{I}}}{A_{\mathrm{Ab}} \cdot U_{\mathrm{I}} + A_{\mathrm{Ap}} \cdot U_{\mathrm{L}} + A_{\mathrm{Ap}} \cdot 4 \cdot \sigma \cdot T_{\mathrm{F}}^3} \qquad (8)$$

The thermal efficiency of the receiver η_{th} is defined by the ratio of the useful heat to the incoming solar radiation in the aperture.

$$\eta_{\mathrm{th}} = \frac{Q}{A_{\mathrm{Ap}} \cdot C \cdot E^{\mathrm{S}}} = F \cdot \alpha - \frac{F \cdot \varepsilon \cdot \sigma \cdot T_{\mathrm{F}}^4}{C \cdot E^{\mathrm{S}}} - \frac{F \cdot U_{\mathrm{L}} \cdot (T_{\mathrm{F}} - T_{\mathrm{a}})}{C \cdot E^{\mathrm{S}}} \qquad (9)$$

The efficiency is plotted for several concentration factors in Figure 4 as a function of the fluid temperature T_{F}.

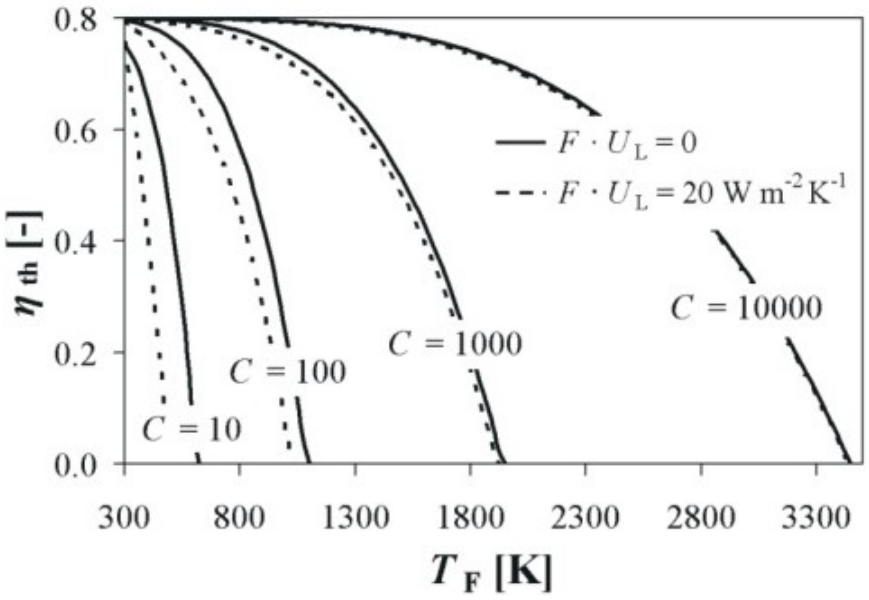

Figure 4: The thermal efficiency of a receiver η_{th} as a function of the fluid temperature T_{F} and the concentration factor C ($F \cdot \alpha = 0.8$, $F \cdot \varepsilon = 0.8$, $E^{\mathrm{S}} = 800$ W m^{-2}, $T_{\mathrm{a}} = 300$ K)

Several messages can be derived from this figure:

- Higher fluid temperatures lead to lower efficiencies
- Higher concentration factors lead to higher efficiencies
- Convection and conduction losses are of minor importance at high concentration factors

Other than for flat plate collectors or parabolic trough receivers the use of transparent covers is not so common in high temperature solar concentrators due to the limited temperature stability and other design constraints of glass covers. In principle it could increase the useful energy gain by a term describing the emission of the hot cover towards the absorber; however, the details of the calculations are complex so that it is referred to the literature (e.g. Winter et al., 1991) here.

Based on Eq. (9), highest efficiencies can be achieved for $\alpha = 1$, $\varepsilon = 0$ and $U_{\mathrm{L}} = 0$. While the latter is of minor importance for high temperature concentrators, the choice of α and ε is crucial. However, an independent and arbitrary selection of both quantities is limited by Kirchhoff's law, which requires that for a specific wavelength λ, the absorptivity equals the emissivity:

$$\alpha(\lambda) = \varepsilon(\lambda) \qquad (10)$$

If the solar spectrum and the spectrum of the emitted thermal radiation are sufficiently different the possibility exists, to make use of the strongly wavelength-dependent characteristics of α to achieve high values of the averaged overall absorptivity α and low values for the average emissivity ε.
In order to find the optimal spectral characteristic for a given high temperature concentrator it is helpful to calculate the radiance temperature T as a function of the wavelength λ of both spectra. $T(\lambda)$ is defined as

$$T(\lambda) = \frac{h \cdot c}{k \cdot \lambda \cdot \ln\left(1 + \frac{2 \cdot \pi \cdot h \cdot c^2}{E_\lambda \cdot \lambda^5}\right)} \qquad (11)$$

where h is the Planck constant, k the Boltzmann constant, c the vacuum light velocity and E_λ the spectral energy density of the radiation. For blackbody radiation the radiance temperature is constant over all wavelengths and equal to the black body temperature.

In Figure 5 the radiance temperature distribution for a real solar spectrum at perpendicular incidence (AM1) is plotted as a function of the wavelength and compared to the radiance temperature of a black absorber at $T_{\mathrm{A}} = 600$ K. In the spectral region where the radiance temperature of the solar spectrum is above of that of the absorber, the emission spectrum should be equal to one, since the gain by solar absorption is higher than the loss by thermal emission. In all other regions the situation is vice versa, so that $\alpha(\lambda) = 0$ is desirable.

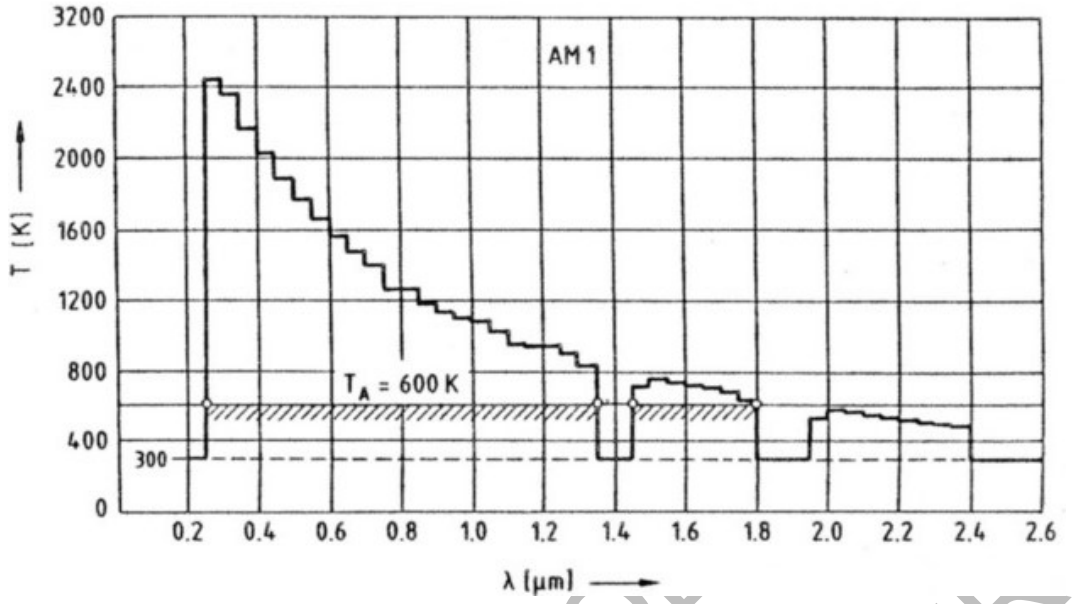

Figure 5: The radiance temperature distribution
(Source: Sizmann et al., 1991. With kind permission of Springer Science and Business Media.)

The spectrum generated by a solar concentrator can be approximated by the spectral emissive power of a black body at a temperature of 5700 K multiplied with the dilution factor f taking into account, that the energy density is reduced due to the large distance of the radiation source:

$$f = \frac{C}{C_{\max}} = \frac{C}{46\,200} = C \cdot 2.165 \cdot 10^{-5} \qquad (12)$$

Applying the concept of the radiance temperature to this distribution and comparing it to radiant black body temperature of the absorber lead to the definition of a cut-off wavelength λ_C where the absorber's absorptivity should fall from $\alpha(\lambda < \lambda_C) = 1$ to $\alpha(\lambda > \lambda_C) = 0$ to achieve the best performance.

Utilizing Figure 6 the efficiency of such a selective absorber can be compared to the efficiency of an ideal black absorber for different concentration factors and as a function of the absorber temperature. Here the convection heat losses are neglected. Based on this figure it can be concluded that selective absorber properties significantly increase the receiver performance, specifically in case of low concentrating systems and high temperatures.

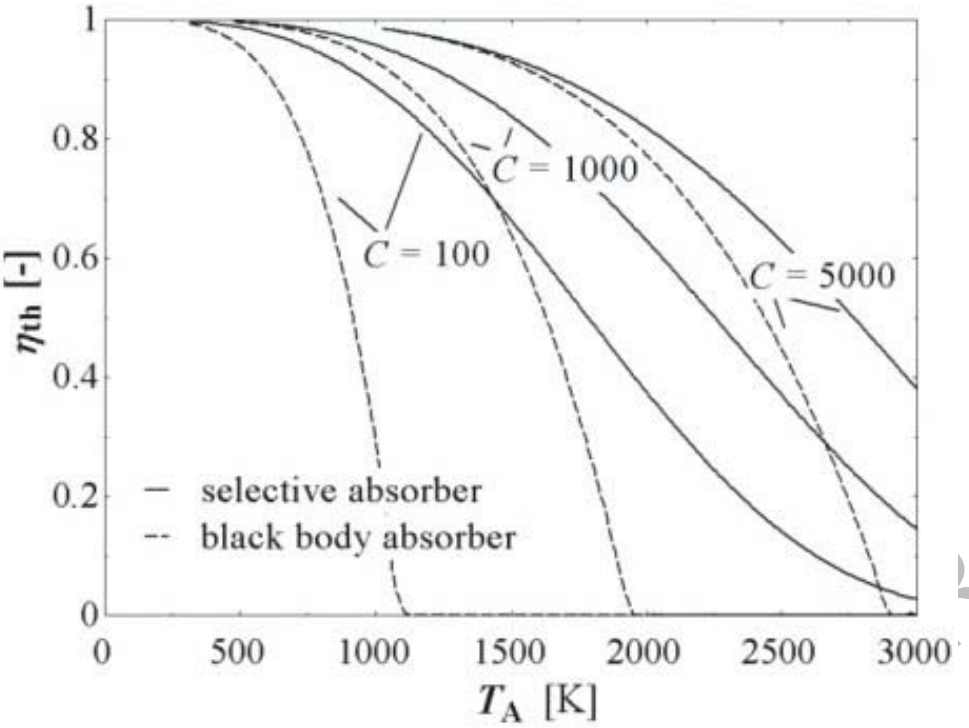

Figure 6: The thermal efficiency of a receiver η_{th} as a function of the absorber temperature T_{A} and the concentration factor C considering the use of a selective absorber and a black body absorber respectively. Convection heat losses are neglected.

In practice selective coatings are only available up to a temperature of 800 K. High temperature stability in atmospheres containing oxygen is still limited, so that today selective coatings are irrelevant for high temperature solar concentrators.

Finally the impact of the heat removal factor F in Eq. (7) has to be discussed. F should ideally be close to 1. This can only be achieved, if the product of the inner heat transfer coefficient U_{I} and the absorber area in Eq. (8) is an order of magnitude larger than the product of the aperture area with the sum of the convective heat loss coefficient U_{L} and the radiation loss coefficient $4 \cdot \sigma \cdot T_{\mathrm{F}}^3$. The latter increases drastically with the temperature. That may pose a severe constraint on F for high temperature solar concentrators for the case that the aperture area and the absorber area are the same.

A possible solution is the use of a cavity receiver. The concentrated radiation enters through a small aperture in a thermally insulated cavity. The actual absorbers are distributed on the inner cavity walls so that the aperture area and the absorber area feature different values. While cavities reduce the problem to achieve sufficiently high F-factors, they destroy the option to benefit from a selective absorber characteristic, due to the inherent characteristics of their apertures approximating a black body, independent of their specific inner surface properties.

2.3. Conversion of Heat to Electricity

In high temperature solar concentrator systems the absorbed energy is often converted into mechanical energy and subsequently to electricity in a power cycle. A part of that cycle is an engine that continuously transfers heat to mechanical energy. Steam or gas turbine cycles are common examples used in fossil power plants to generate electricity from the heat input provided by the combustion of fuels. Thermodynamic principles forbid that all heat input is completely transferred to electricity, because part of it must be removed at a lower temperature level.

In a generic power cycle a working fluid undergoes a number of changes of its state repeated in a cycle. In order to force the system from one state to the next heat or work must be delivered to or extracted from the fluid. Depending on the kind of working fluid and the state changes many different power cycles can be set up. A very famous example is the Carnot cycle, an idealized reversible process that consists of two isothermal (2→3 and 4→1) and two isentropic (1→2 and 3→4) changes of state. In Figure 7 the corresponding *T*/*s*-representation is shown, where *s* is the specific entropy of the fluid.

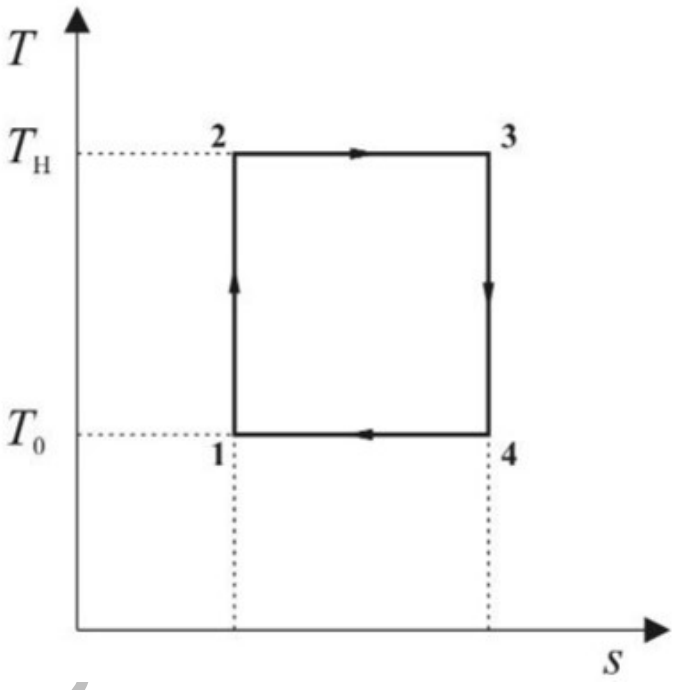

Figure 7: *T*/*s*-representation of the Carnot cycle

At the upper temperature T_H the fluid receives heat and at the lower temperature T_0 heat is released. The cycle efficiency η_C describing the fraction of heat input Q_{in} that is converted to work W is independent of the working fluid and can be calculated as

$$\eta_C = \frac{W}{Q_{in}} = 1 - \frac{T_0}{T_H} \qquad (13)$$

It can be shown that the Carnot cycle efficiency is equal to the theoretical maximum efficiency of any heat to mechanical energy conversion process. As a consequence of this equation heat input should be provided at a very high temperature whereas heat removal should occur close to the ambient temperature to achieve high conversion efficiency. For the application of heat engines in high temperature solar concentrator systems it should be kept in mind that the efficiency of a solar receiver drops with increasing temperature (see Figure 6). The product of both efficiencies

$$\eta_{\text{tot}} = \eta_{\text{C}} \cdot \eta_{\text{th}} \qquad (14)$$

is considered to be the relevant quantity to describe the performance of an ideal solar high temperature concentrator system that produces electricity postulating an efficiency of 100 % for the conversion of mechanical power to electricity. In Figure 8 η_{tot} is plotted as a function of the absorber temperature. Several graphs based on different concentration factors C and different absorber characteristics (selective or black body type as presented in Figure 6) are shown. For this calculation the upper fluid temperature is assumed to be equal to the absorber temperature. Obviously, there is an optimum temperature for each concentration ratio where the maximum performance can be achieved. The higher the concentration ratio is, the higher is the optimal temperature and the higher is the theoretical conversion efficiency. Although selective surfaces are not available for temperature beyond 800 K today, Figure 8 suggests that there is a potential in efficiency increase for further developments.

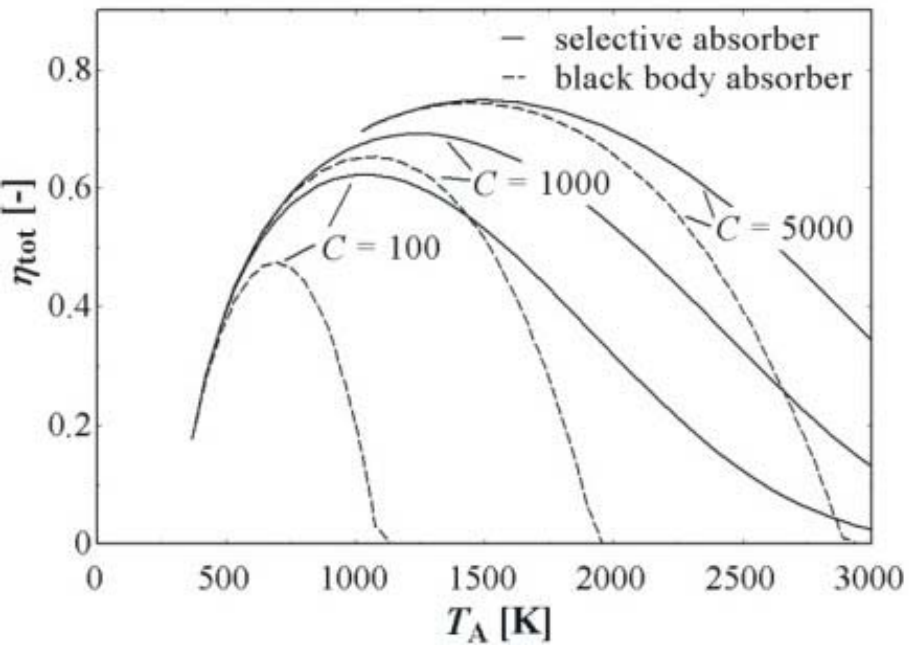

Figure 8: Theoretical total efficiency of a high temperature solar concentrating system for the generation of mechanical work as the function of the upper receiver temperature for different concentration ratios and an ideal selective or a black body characteristic of the absorber

In practice the optimal operation temperatures will deviate from these theoretical figures, because power cycles with Carnot performance do not exist in reality. It also has to be considered that such systems are often operated under part load conditions which also impacts the efficiency of the system.

Today, power cycles are not specifically developed and optimized for high temperature solar concentrating systems but conventional fossil fuel driven power generation systems are adapted to the solar applications. The most relevant ones are steam turbine cycles, gas turbine cycles and Stirling engine cycles, which will be discussed subsequently.

Steam turbine cycles

Steam power plants are based on the Clausius-Rankine Process using water/steam as the working fluid. A schematic of the cycle is shown in Figure 9 and the associated *T*/*s*-representation in Figure 10.

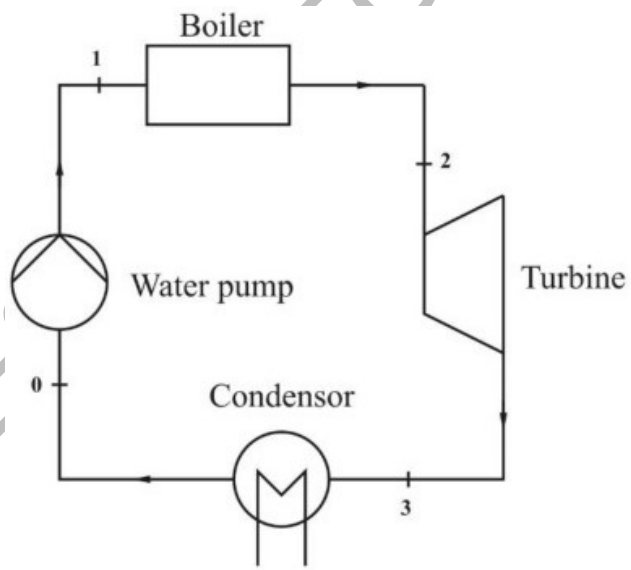

Figure 9: Schematic of the Clausius-Rankine Process

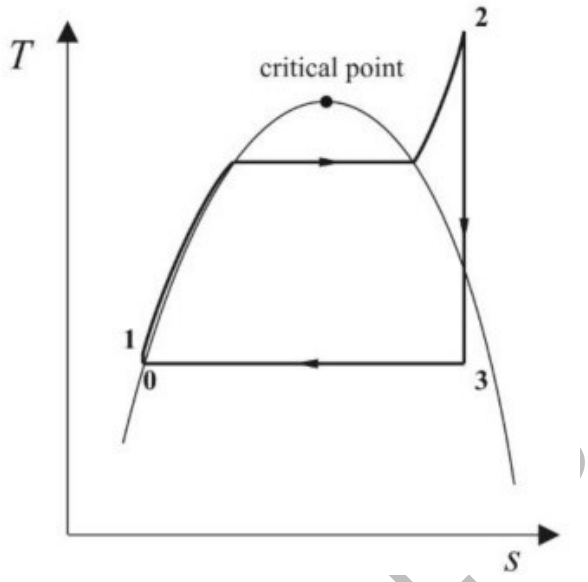

Figure 10: *T*/*s*-representation of the Clausius-Rankine Process

Heat is provided to water along a supercritical isobar in a boiler (1→2); work is extracted during an isentropic expansion in a turbine (2→3); heat is removed in the wet steam region along the overlapping isobar and isotherm in a condenser (3→0). Finally condensed water is isentropically compressed in a feed water pump (0→1). The theoretical cycle performance can be calculated by Carnot's equation if the following definition for the average temperature T_m is used as the value for the upper process temperature in Eq. (13).

$$T_m = \frac{h_2 - h_1}{s_2 - s_1} \qquad (15)$$

The relevant conditions of the working fluid are condition 1 and condition 2, which correspond to its conditions before entering and after leaving the boiler. The variable h represents the specific enthalpy of the fluid.

The heat input in a Rankine cycle is not required at a constant temperature but the heating of the working fluid fits excellently to the temperature change of the combustion gas in the boiler, so that it can be more efficiently adapted to fossil fuel operation compared to the Carnot cycle. The same benefit also holds for high temperature solar concentrator applications where a secondary sensible heat transfer fluid is used to transfer the absorbed solar heat to the primary working fluid of the cycle. However, if the primary working fluid would be heated up by solar radiation directly, also isothermal heat input could be realized by the solar system, since the heat input takes place by radiation. This opens up options for future cycle optimizations in solar applications.

The operation in a real steam power plant deviates from the ideal Clausius-Rankine cycle in a number of points. To reduce the thermal and mechanical load to the material, pressure and temperature are limited to values below the values resulting from

thermodynamic optimizations. In addition measures of internal heat recovery are used to increase the average temperature of heat input to the upper steam temperature. Today, upper temperatures of the steam turbine cycle are limited to approximately 650 °C (which corresponds to $T_m \approx 580\,°C$) due to material constraints. In the near future 700 °C may be feasible. A comparison with Figure 8 reveals that for selective receivers real steam cycles are best suited for concentration factors below 100. If selective absorbers are not available, concentration factors between 100 and 1000 are appropriate. However, beyond a concentration of 1000, a steam cycle is not a good choice to be combined with high temperature solar concentrators, because they could not exploit the elevated temperature levels in practice. The electric power output of today's steam turbine systems ranges from a few MW to several hundred MW.

Gas turbine cycles

Gas turbine systems are based on the Brayton cycle using an ideal gas as the working fluid. A schematic of the cycle and its *T*/*s*-representation are shown in Figure 11 and 12 respectively.

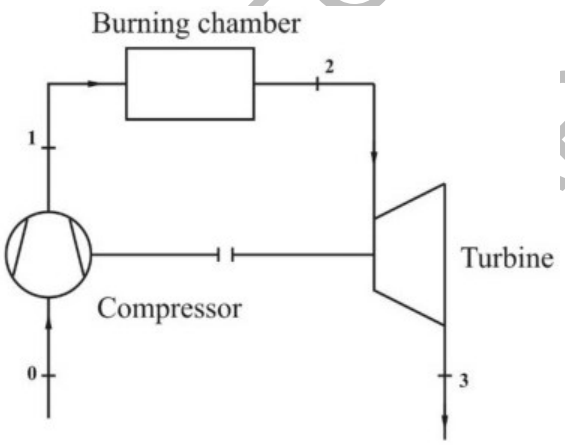

Figure 11: Schematic of the Brayton Process

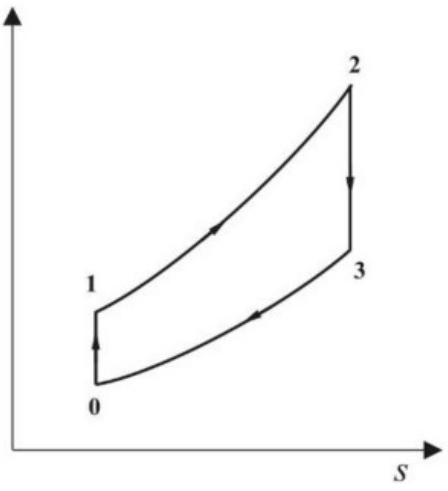

Figure 12: *T*/*s*-representation of the Brayton Process

The fluid is isentropically compressed in a compressor (0→1). Heat is provided to the gas being in use along an isobar in a burning chamber (1→2); work is extracted during an isentropic expansion in a turbine (2→3); heat is removed when the working fluid is released to the ambient (or in closed cycles through an external heat exchanger). The efficiency of that ideal cycle does not reach the Carnot efficiency in particular, because the fluid leaves the turbine at a temperature level significantly above the ambient temperature. Improvements can be achieved if heat recovery measures are used. The performance also depends on the properties of the working fluid. Using helium instead of air would on the one hand allow a higher performance, but on the other hand require heat removing from the system through a heat exchanger, whereas air could be used in an open cycle. Turbine inlet temperatures in modern gas turbine can exceed 1300 °C. The turbine exit temperatures range between 500 °C and 600 °C. Although the temperature level in gas turbines is significantly higher than in steam turbines the achievable efficiency is below that of modern steam turbine systems, because of the high heat removal temperature. Gas turbines bear the advantage that they are built much more compact, can be operated very dynamically and do not need additional heat exchangers to remove the heat from the process when operated in an open cycle. Furthermore they are operated at significantly lower pressure levels (5 bar to 30 bar) compared to steam turbines (100 bar to 200 bar) which reduces the costs of the system very much. Gas turbine systems are available in the power range form 100 kW to several 100 MW of electric power output.

Considerable improvements in the performance of such a system can be achieved, if the rejected heat of the gas turbine is recovered and used in a subsequent Rankine Cycle. This is done in practice by an air to steam heat exchanger that transfers the waste heat of the turbine exhaust gases to the water/steam working fluid. This concept is often referred to as *combined cycle* power plant and has reached the highest performance of fuel based power cycles approaching an efficiency of 60 % for natural gas fired systems. Since the upper process temperature in the gas turbine exceeds 1500 K, this concept appears to be attractive to be applied in high temperature solar concentrators attaining concentration factors beyond 1000.

Stirling Engine

The Stirling engine was patented in 1816 by the Reverend Robert Stirling. It is a hermetically sealed piston engine that works by the repeated heating and cooling of an amount of working gas, usually air or other suitable gases such as hydrogen or helium. The *T*/*s*-representation of the Stirling cycle is shown in Figure 13.

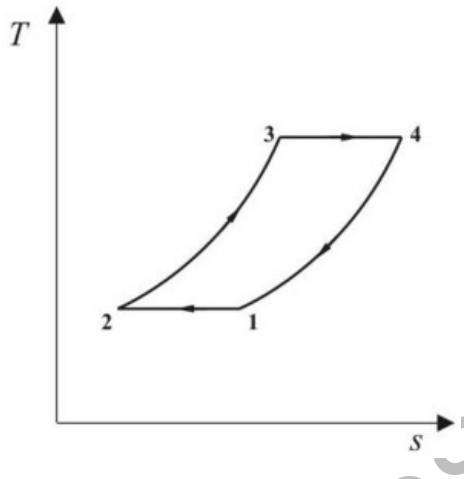

Figure 13: *T*/*s*-representation of the Stirling cycle

In the idealized Stirling cycle heat (i.e. energy) is transferred to the working fluid within the sequence 2→3→4. Conversely, heat (energy) is extracted from the working fluid during the sequence 4→1→2. In the segment 2→3, an isochoric change of state, heat is transferred to the fluid internally via regeneration of the energy removed from the fluid in segment 4→1 along an isochore. That means that (ideally) heat is added from an external source only during the isothermal sequence 3→4 and that heat is rejected to the surrounding environment only in the isothermal segment 1→2. The major challenge concerning the Stirling cycle is related to the internal heat exchange.

Different concepts of a Stirling engine have been proposed, e.g. the so called alpha type Stirling. An α-Stirling contains two different cylinders and accordingly two separate pistons, a "hot" piston, the power piston, and a "cold" piston, the compression piston. The hot piston is situated in the cylinder next to the high temperature heat exchanger and the cold piston is located in a cylinder, which is connected to the low temperature heat exchanger. The regenerator is mounted between the two heat exchangers. In the following the ideal Stirling process is visualized employing a design which is similar to the alpha configuration Stirling engine (cf. Figure 14).

Process 1→2: Isothermal compression – the compression piston (CP) moves inward and performs work W_C on the system in order to compress the working gas. The heat Q_C is rejected by the (external) low temperature heat exchanger in order to keep the gas temperature constant.

Process 2→3: Isochoric heating – the power piston (PP) moves together with the compression piston transferring working gas (via the regenerator and heat-exchangers) from the cold to the hot end of the machine. The heat Q_R is applied to the working gas as it passes through the regenerator. The gas temperature raises, finally reaching that of the high temperature heat exchanger. Simultaneously the gas pressure increases significantly.

Process 3→4: Isothermal expansion – the high-pressure working gas expands and work W_E is performed on the power piston as it moves outward. Due to the external heat input Q_E the gas temperature does not fall.

Process 4→1: Isochoric cooling – the power and compression pistons move together transferring the working gas (via the regenerator and heat-exchangers) back to the cold end of the machine. The heat Q_R is extracted from the working gas as it passes through the regenerator. The gas temperature does not change since the gas pressure decreases in an analogous way.

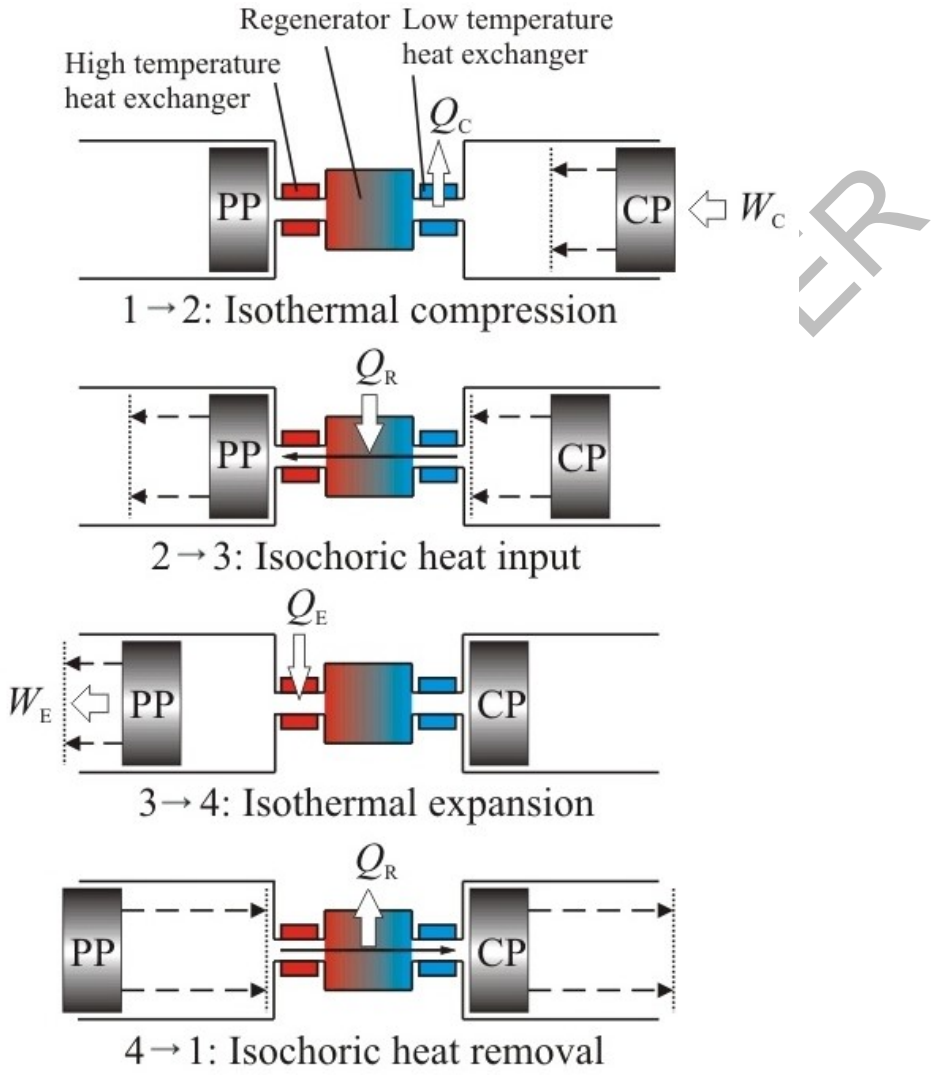

Figure 14: The basic operations of an α-like Stirling engine

In a real engine, the changes of states can not be separated into these four changes of state but they can be described by a combination of them.

Some Stirling engines rely on a separate electric generator or alternator to convert the mechanical power into electricity, while others have an integrated alternator. The

resulting engine/alternator-system with its ancillary equipment is often called a converter or a power conversion unit. The motion is accomplished – as described above – by moving the gas between hot and cold heat exchangers, the hot heat exchanger being a chamber in thermal contact with an external heat source, e.g. a fuel burner or a solar receiver, and the cold heat exchanger being a chamber in thermal contact with an external heat sink, e.g. cooling fins. The heat-exchange process provides near-ideal efficiency concerning the conversion of heat into mechanical energy by following the Carnot cycle as closely as practically possible with given materials. Due to its high performance and because of the fact that an isothermal heat input is required by a Stirling cycle which can be effectively given by radiation energy, it is of particular interest to combine this engine with a high temperature solar concentrator. Today's high temperature Stirling engines are available in a power level of some 10 kW of electric output.

The highly-efficient Stirling engine is the leading candidate to be used in power systems based on solar parabolic dish concentrators. The Stirling engine's efficiency increases with the hot end temperature, hence it is a goal to operate engines at a temperature being as high as possible. Operation temperatures are constraint by the thermal limits of the material and not by the solar concentrator, because temperatures beyond the operating capabilities of existing engines are easily obtained by solar concentration. Stirling engines therefore generally operate at the thermal limits of the materials used for their construction. Typical temperatures range from 650 °C to 800 °C resulting in engine conversion efficiencies of around 30 % to 40 %.

Following from their good heat-transfer characteristics hydrogen and helium have been used as the working gas for dish/Stirling engines. Hydrogen, thermodynamically a better choice, generally results in more efficient engines than helium does. Helium, on the other hand, has fewer material compatibility problems and is not inflammable, an important point of safety.

To maximize power, engines typically operate at high pressures, in the range of 50 bar to 200 bar. Operation at these high gas pressures makes gas sealing difficult: seals between the high pressure region of the engine and those parts at ambient pressure have been problematic parts in some engines. New designs to reduce or eliminate this problem are currently being developed.

Engine designs for dish/Stirling applications are usually categorized either as kinematic or as free-piston systems. The power piston of a kinematic Stirling engine is mechanically connected to a rotating output shaft. If there is a separate gas displacer piston, it is also mechanically connected to the output shaft.

The power piston of a free-piston Stirling engine is not mechanically connected to an output shaft. It bounces alternately between the space containing the working gas and a spring (usually a gas spring). In most designs, the displacer piston is also free to bounce on gas or mechanical springs. The piston frequency and the timing between the two pistons are established by the dynamics of the spring/mass system. To extract power, a magnet is attached to the power piston and electric power is generated as it moves past

stationary coils. Other schemes for extracting power from free-piston engines, such as driving a hydraulic pump, have also been considered.

To make a dish/Stirling engine system economical, a system lifetime of at least 20 years with little maintenance is generally required. The duration of electric power production should reach about 40 000 to 60 000 hours – approximately 10 times more than the lifetime of a typical automotive internal combustion engine. If a major overhaul of the Stirling engine, including replacement of seals and bearings, is necessary within the lifetime, operating costs will increase noticeable. An important challenge, therefore, is to enhance the design of dish/Stirling engines reducing the potential of wear in critical components or creating parts which are insusceptible to negative effects.

3. Technical Concepts

3.1. Parabolic Dishes

A solar dish/Stirling electric power generation system is one option for a high temperature solar concentrator that is capable to achieve a high system performance. This results from the fact that it combines an excellent concentrator, a very efficient cavity receiver and a high performance heat engine. Such systems have demonstrated a solar to electric power efficiency of close to 30 %.

A dish/Stirling system consists of the following components:

- A sun-tracking system rotates the solar concentrator about two axes to keep its optical axis pointing directly toward the sun. The concentrator's shape allows reflecting the sun's rays into a cavity receiver located at the focal spot.
- The cavity receiver absorbs the concentrated solar energy. Thermal energy then heats the working gas in the Stirling engine.
- The Stirling engine converts the heat into electricity.

The size of the solar collector (i.e. concentrator) of dish/Stirling systems is determined by the power output desired at maximum insolation levels (nominal 1000 W m^{-2}) as well as the collector and power-conversion efficiencies. With current technologies a 5 kW_e dish/Stirling system requires a dish of approximately 5.5 m in diameter whereas for a 25 kW_e system the installation of a dish of about 10 m in diameter is necessary.

Thin glass mirrors with a silvered back surface have been used in the past as reflectors. Some current designs use thin polymer films with aluminum or silver creating a reflective surface.

The ideal shape for the reflecting surface of a solar concentrator is a paraboloid. In practice, however, it is often easier to fabricate multiple spherically shaped surfaces. Spherically shaped surfaces also concentrate solar radiation when the focal spot is many mirror diameters away from the reflecting surface (i.e. the mirror is only slightly curved), because the parabola can be well approximated in such a small section.

Some concentrators for dish/Stirling systems use multiple spherically shaped mirror facets supported by a truss structure (see Figure 15), with each facet individually targeted in order to approximate a paraboloid. This approach to concentrator design makes very high focusing accuracy possible.

Figure 15: Faceted parabolic dish concentrator with truss support (Courtesy of SES)

A recent innovation in solar concentrator design is the use of stretched membranes. Here, a thin reflective membrane is stretched across a rim (or hoop) and a second membrane is used to close off the space behind. A partial vacuum is drawn in this space, bringing the reflective membrane into an approximately spherical shape. If many facets are used (as shown in Figure 15), their focal region will be a number of facet diameters away and the spherical shape of the facets provides an adequate solar concentration for dish/Stirling applications.

If only one or a few stretched membranes are used (see Figure 16), the surface shape should approximate a paraboloid. This approximation can be achieved by initially forming a paraboloid-like shape with the membrane and using the pressure difference between front and back to support the surface and maintain its shape.

Figure 16: The stretched-membrane parabolic dish concentrator Distal II(Source: PSA, 2004)

In order to track the sun, concentrators must be capable of moving about two axes. Generally, there are two ways of implementing this, both having advantages:

- Azimuth-elevation tracking: the dish rotates in a plane parallel to the earth (azimuth) and in another plane perpendicular to it (elevation). This gives the collector up/down and left/right rotations. Rotational rates about both axes vary throughout the day but are predictable. The faceted concentrator shown in Figure 15 and the stretched-membrane concentrator shown in Figure 16 use an azimuth-elevation tracking mechanism.
- Polar tracking: the collector rotates about an axis parallel to the earth's axis of rotation. The collector rotates at a constant rate of 15 degrees per hour, the same rotation rate as the earth's one. The other axis of rotation, the declination axis, is perpendicular to the polar axis. The movement about this axis occurs slowly and varies by +/- 23.5 degrees over a year (with a maximum rate of 0.016 degrees per hour).

The concentrated radiation – the sun's image from the concentrator can be well approximated by a Gaussian profile – is directed onto a receiver, which has two functions: (1) to absorb as much as possible of the solar radiation reflected by the concentrator and (2) to transfer this energy as heat into the engine's working gas.

Receivers for dish/Stirling systems are cavity receivers with a small opening (aperture) through which concentrated sunlight enters. The absorber is placed behind the aperture to limit the flux density on the absorber. The insulated cavity between the aperture and

the absorber decreases the amount of heat lost. The receiver aperture is optimized to be just large enough to admit most of the concentrated sunlight but small enough to limit radiation and convection losses (cf. Stine et al., 1985).

In a receiver, two methods are used to transfer absorbed solar radiation to the working gas of a Stirling engine. In the first type of receiver, the directly illuminated tube receiver, small tubes through which the engine's working gas flows are placed directly in the concentrated solar flux region of the receiver (see Figure 17). These tubes form the absorber surface.

Figure 17: The Eurodish-receiver, an example of a directly illuminated tube receiver (Courtesy of SOLO Stirling GmbH)

Heat-pipe receivers use sodium or a mixture of sodium and potassium to transfer heat from the surface of the receiver to the engine heater head. Heat pipes utilize a capillary wick to distribute the liquid metal over the back surface of the absorber. The liquid metal evaporates, vapor is transported to the engine heater head, where it condenses, and the liquid metal refluxes to the absorber. In these receivers, the liquid metal condenses at a constant temperature thereby providing an uniform heating to the Stirling engine. In contrast direct irradiation receivers can experience large temperature differences in different parts of the aperture or along the tubes of the receiver. The receiver materials typically limit the peak receiver temperature and thus the performance. In a heat pipe receiver the peak temperature is the average temperature, which raises the achievable working gas temperature considerably. The increased working gas temperature, improved receiver efficiency, improved temperature balance

among the four cylinders of the engine and overall simplicity resulted in a 20 % increase in system efficiency.

Figure 18 shows the daily generated electric energy based on the daily sun input for different concentrating technologies. The more output a system can provide at a given solar input, the higher is the system performance. Dish/Stirling systems show the best characteristics, due to their high concentrator and engine performance and due to their low thermal inertia which allows for a quick start-up compared to large-scale concentrating solar power systems like central receivers as discussed in the subsequent section or parabolic troughs not dealt with in this work.

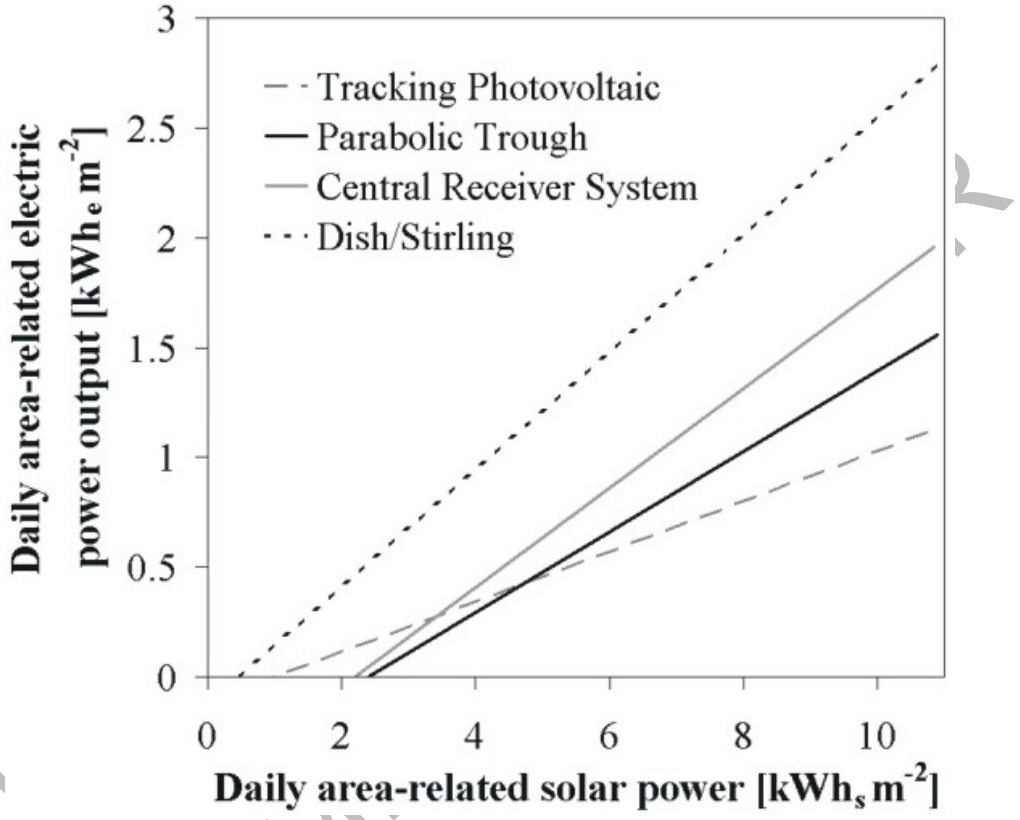

Figure 18: Performance of different solar systems
(Source of data: Southern California Edison and Sandia National Laboratories)

A detailed insight into the different losses can be extracted from a typical waterfall chart (see Figure 19). The incident power is reduced by imperfect reflection, by radiation that misses the cavity aperture (intercept), by heat losses of the receiver, by conversion losses of the Stirling engine, by losses in the electrical generator and finally by parasitic power requirements needed to operate pumps and motors.

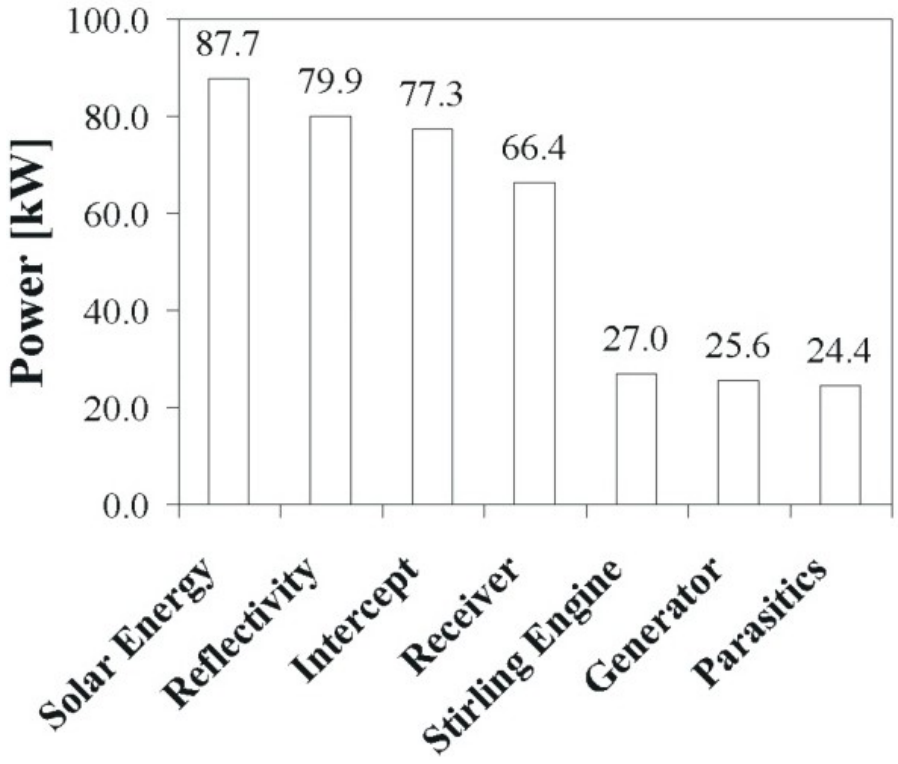

Figure 19: Waterfall chart of the SES System (cf. Mancini et al., 2003)

Table 1 gives an overview of the technical specification of four current dish/Stirling systems under commercial deployment.

	SAIC / STM [a] System	SBP [b] System	SES [c] System	WGA [d] (Mod 1) ADDS [e] System	WGA (Mod 2) Remote System
Concentrator					
Type	approximate	paraboloid	approximate	paraboloid	paraboloid
Number of facets	16	12	82	32	24
Glass area [m^2]	117.2	60	91	42.9	42.9
Projected area [m^2]	113.5	56.7	87.7	41.2	41.2
Reflectivity [-]	0.95	0.94	0.91	0.94	0.94
Height [m]	15	10.1	11.9	8.8	8.8
Width [m]	14.8	10.4	11.3	8.8	8.8
Weight [kg]	8172	3980	6760	2864	2481
Track control	open / closed loop	open loop	open loop	open / closed loop	open / closed loop
Focal length [m]	12	4.5	7.45	5.45	5.45
Intercept factor [-]	0.9	0.93	0.97	0.99+	0.99+
Peak value of energy density [kW m^{-2}]	2500	12 730	7500	> 11 000	> 13 000
Power conversion unit					
Aperture diameter [m]	0.38	0.15	0.2	0.14	0.14
Engine manufacturer / type	STM 4-120	SOLO 161	Kockums / SES	SOLO 161	SOLO 161
	double acting kinematic	kinematic	4-95 kinematic	kinematic	kinematic
Number of cylinders	4	2	4	2	2
Displacement [cm^3]	480	160	380	160	160

Operating speed [min^{-1}]	2200	1500	1800	1800	800–1890
Working fluid	hydrogen	helium	hydrogen	hydrogen	hydrogen
Power control	variable stroke	variable pressure	variable pressure	variable pressure	variable pressure
Generator	3 φ / 480 V / induction	3 φ / 480 V / induction	3 φ / 480 V / induction	3 φ / 480 V / induction	3 φ / 480 V / synchron
System information					
Number of systems built	5	11	5	1	1
Operational time [h]	6360	40 000	25 050	4000	400
Power rating [kW]	22	10	25	9.5	8 [f]
Peak net output [kW]	22.9	8.5	25.3	11	8
Peak net efficiency [%]	20.0	19 [g]	29.4	24.5	22.5
Annual net efficiency [%]	14.5	15.7	24.6	18.9	no data [h]
Annual energy production [kWh]	36 609	20 252	48 129	17 353	no data

[a] Science Applications International Corp. / STM Power, Inc.

[b] Schlaich-Bergermann und Partner / Other members of the EuroDish project: MERO, Klein+Stekl, Inabensa, Deutsches Zentrum für Luft und Raumfahrt (DLR - Germany), Centro de Investigaciones Energéticas Medioambientales y Tecnológicas (CIEMAT - Spain)

[c] Stirling Energy Systems

[d] WGAssociates

[e] Advanced Dish Development System

[f] "The Mod 2 ADDS drives a conventional submersible water pump. The test pump is undersized for the output of the system. Therefore, mirror covers are used to limit output to the pump capacity."

[g] "The SBP system peak efficiency is calculated at its design point of 800 W/m^2. All other system efficiencies are calculated at their design points of 1000 W/m^2."

[h] "The Mod 2 system has not operated for 1000 hr."

Table 1: Comparative specifications and performance parameters for dish/Stirling systems (cf. Mancini et al., 2003)

To date dish/Stirling systems have a prototype status. The electricity generation costs are still significantly above that of large-scale central receiver or parabolic trough power plants. They have successfully demonstrated that they can produce electrical power for extended periods of time. The major technical issue is to establish high levels of system reliability and thereby to reduce the operating and maintenance costs. The second barrier to the market entry is the initial cost of the systems, that, to a large extent, depends on the production levels of the components and the systems. It may decrease sharply in the near future, since SES and a Californian utility have signed a contract to provide grid power by a park installation of dish/Stirling systems. A capacity of 500 MW (20 000 units) is intended for the implementation started in 2009 and completed in 2012.

3.2. Central Receiver Systems

A central receiver system (CRS) is another concept for a high temperature solar concentrator that aims at the collection of large amounts of highly concentrated solar energy without requiring a piping. In this concept it is expected to achieve economy-of-scale benefits, because systems with several 100 000 m^2 of reflector surface area can focus to a single receiver approaching several 100 MW of power and thus use conventional power plant technology for the power cycle.

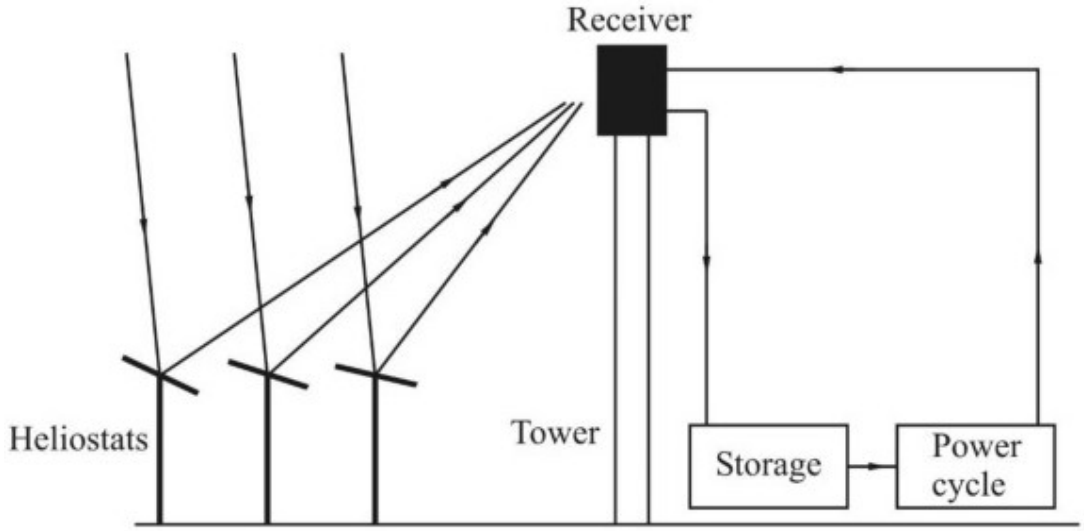

Figure 20: Central receiver system (CRS)

A CRS consists of the following components (see Figure 20):

- a large number of two axis tracking mirrors called heliostats (each one of a size comparable to a dish concentrator described in the previous paragraph) that concentrate the solar radiation onto one common area, normally located on the peak of a central tower,
- the receiver system at the top of the tower, where the energy is absorbed and transferred to a heat transfer fluid,

- a power cycle to generate electricity (typically steam cycles are used but experiments with gas turbine cycles have also been made) and
- a thermal energy storage which allows running the power cycle system during non-sunshine hours if charged before (option).

A CRS can be distinguished by a number of criteria. The most relevant appears to be the heat transfer fluid (which is often linked to the desired outlet temperature). Experiences have been collected with water or rather steam, liquid sodium, liquid nitrate salt and air (atmospheric and pressurized). All concepts are under further development – some including an initial commercial deployment phase – with the exception of sodium, due to the hazardous experience of a sodium fire in a test system in Almería in 1986.

The components are described in detail in the following.

Heliostats (cf. Mancini, 2000)

The word Heliostat comprises helio for sun and stat for the fact that the reflected solar image is maintained at a fixed position over the course of the day. They are nearly flat mirrors (some curvature is required to focus the sun's image) that collect and concentrate the solar energy on a tower-mounted receiver located 100 m to 1000 m distant. A 100 MW_e CRS would require nearly one million m^2 of glass heliostats, corresponding to approximately 10 000 100-m^2 heliostats. The heliostats represent 40 % to 50 % of the cost of a power tower; consequently they must be relatively low-cost so that the cost of electric power from such a plant can compete with the respective cost of fossil fuel power plants.

The major components of a heliostat – described briefly below – are the mirror assemblies (typically glass and metal), the support structure, the pedestal and foundation, the tracking control system, and the drives. Most of the mentioned components are shown in Figure 21. The mirror surfaces of state-of-the-art heliostats are made with thin silvered glass, which may have a low iron content causing an enhanced reflectance, a higher resistance to oxidation and therefore a better durability. Aluminum and silver coated polymer films have been under development for solar applications for some time, but these materials have not yet demonstrated the ability to survive 20 to 25 years which are required for power plant applications. In order to provide the proper contour for the optical surface and for attachment to the support structure, the glass may be bonded or otherwise joined to a metal, honeycomb or slumped-glass substrate that has been "shaped" to the proper curvature. The optical element support structure positions the mirrors accurately and carries the weight of the structure as well as wind loads through the drives to the ground. For a heliostat, it is important that the mirror facets are located relatively to one another so that each of their images is focused on the receiver at the top of the tower. The major issues that a heliostat designer must confront are these two requirements: maintaining mirror alignment and providing structural strength. By far the most common type of ground support for solar concentrators is the poured in-place tubular pedestal. This is, however, not the only type of tracking structure that has been used for heliostats. Alidade-type structures with pintel bearings and polar tracking structures have also been utilized. Tracking controls are the electronics and control algorithms that are used to provide the

drive motors for maintaining the position of the concentrator relative to the sun with the needed signals. Heliostats must always track a point in the sky that is located midway between the receiver and the sun in order to reflect their images onto the receiver. The concentrator drive causes the heliostat to move about two axes, azimuth and elevation, to picture the sun's image at a predetermined location on the tower. The drive does not only provide the tracking but it must also carry the weight of the concentrator and any wind loads to the ground through the pedestal and foundation.

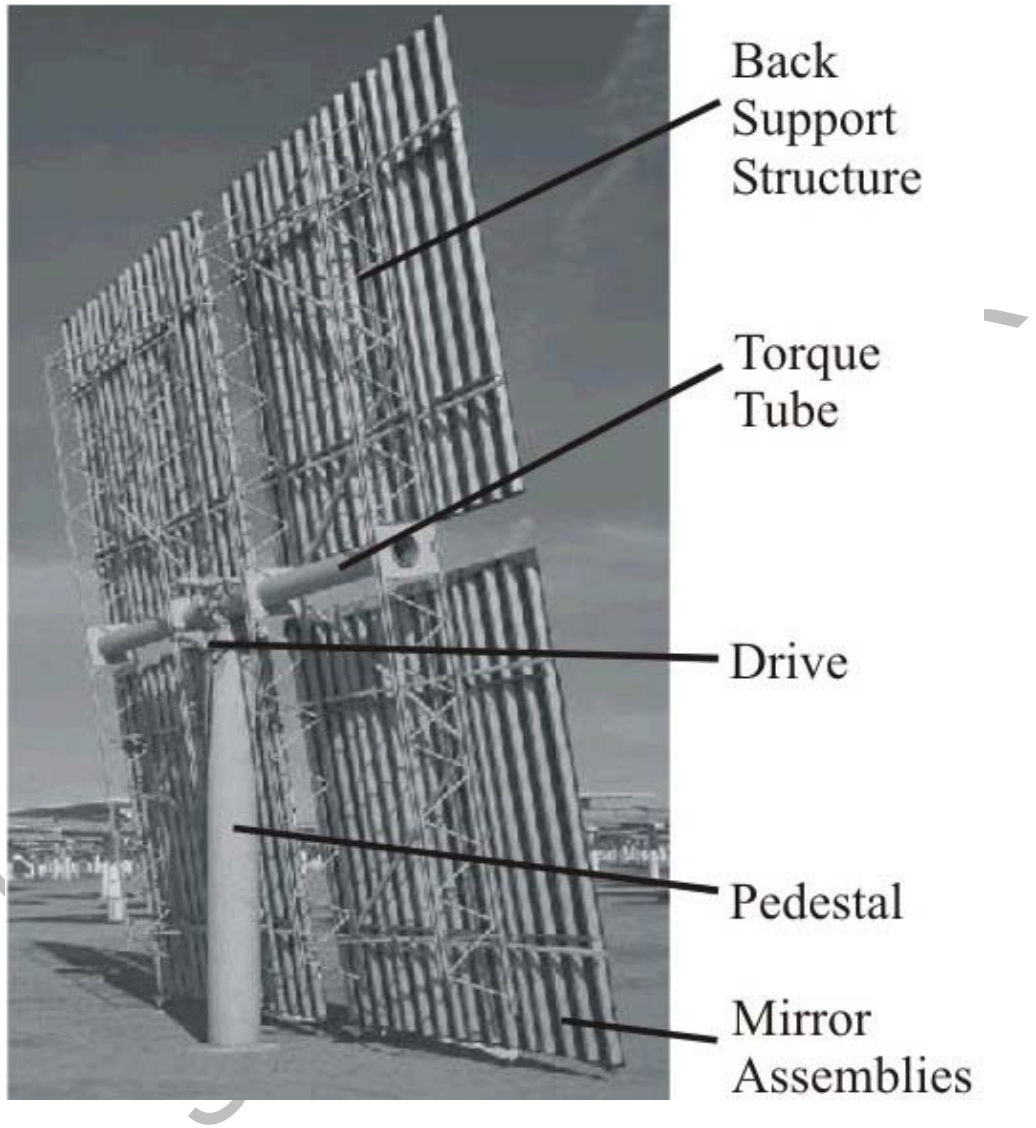

Figure 21: Major components of a heliostat (Source of photography: Mancini, 2000)

Heliostat Field

The collectivity of heliostats located around the central tower is called the heliostat field. It represents a Fresnel-type concentrator. Since all heliostats are situated in the same plane they do not approximate one single parabola but each individual heliostat approximates a segment of a separate parabola. Thus, the achievable concentration ratio of CRSs is significantly lower than that of parabolic dish systems, reaching values of

500 to 1500 in practice. Terminal non-imaging CPCs (cf. Section 2.1.) may be used to boost the concentration further.

The positioning of heliostats around the central tower requires a complex optimization process that depends mainly on the latitude of the site, the needed concentration, the power level and the quality as well as the size of the heliostats. It can be distinguished between a north field configuration, where heliostats stand only on one side of the tower (northwards in the northern hemisphere) to reflect the radiation to a southward direction aiming at the receiver at the top of the tower, and a surround field, where heliostats around the tower reflect the radiation to a cylindrical receiver or a number of individual receivers facing various directions. Which one of the both options is favored depends on the relative impact of two compensating effects:

- Heliostats to the north of the tower (for the northern hemisphere) can reflect more energy back to the tower because their projected area towards the sun is larger than for southern heliostats which have to be aligned much differently to reflect the radiation "backwards overhead" to the tower. This effect is called "cosine loss".
- The greater the distance between the heliostat and the tower the higher the losses due to atmospheric attenuation and the fraction of radiation that misses the receiver.

Thus, southern heliostats that are located close to the tower may provide more energy than northern heliostats that stand very far away despite their higher cosine losses. This leads to the fact, that for northern latitudes and for small power levels a northern field is the optimal choice whereas for sites closer to the equator and for larger power levels surround fields achieve a higher annual energy yield.

A special configuration of a CRS is the combination of a heliostat field with a tower reflector that redirects the radiation back to the ground. Although further reflections imply additional losses, it offers the benefit to avoid extensive piping of hot fluids and to locate heavy components like receiver, power cycle, and storage very close together on the ground. An obvious difficulty is that for the practical design the tower-top reflector area must be much (5 to 100 times) smaller than that of the heliostat field itself to make sense at all. Thus the tower reflector must tolerate a flux density of 5 to 100 times the density of the incident solar radiation that may lead to overheating problems. The most rational design is based on the Cassegranian optics (see Figure 22): a hyperbolic reflector below the focal point of the heliostat field, which is significantly smaller than a flat mirror reflector half-way between heliostat reflector plane and heliostat focus point. However, due to its hyperbolic shape the reflector magnifies the image of the heliostat field, and thus reduces the concentration factor. A further terminal concentrator may be used compensating the aforementioned effect but also adding losses and causing extra costs.

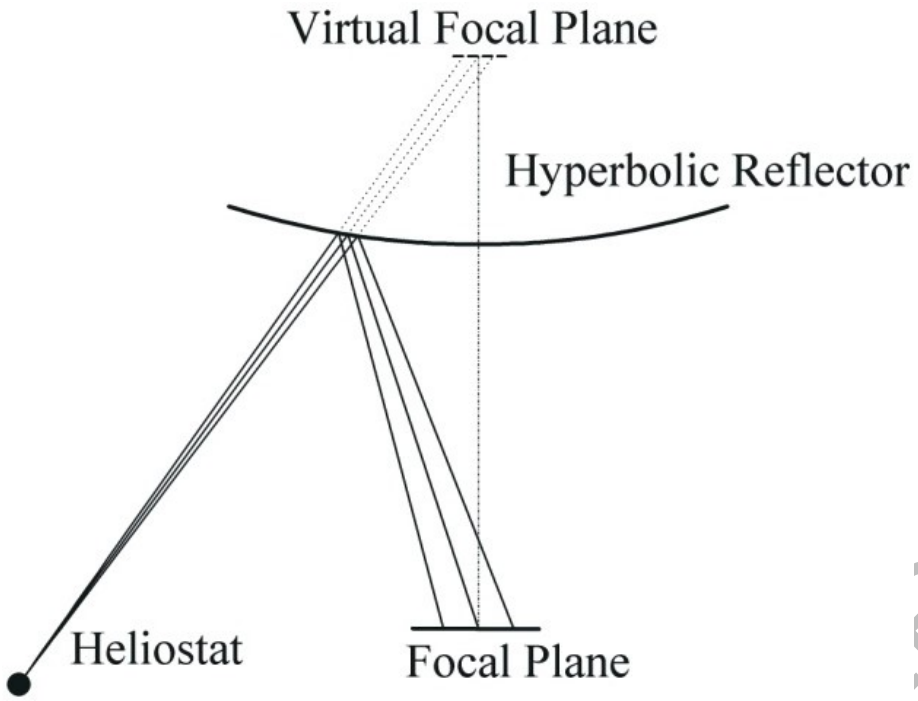

Figure 22: Hyperbolic reflector concept

Receiver

There are two different receiver designs in CRSs, the external and the cavity design. In cavity receivers, the heat absorbing elements are located inside of an insulated cavity. The focal spot of the heliostat field coincides with the aperture of the cavity. In external receivers the heat transferring surfaces are exposed to the ambient and are located directly in the focal point of the heliostat field. Cavity receivers offer the benefit of lower heat losses but generally constrain the direction of the incoming radiation and thus impact the heliostat field arrangement. They also restrict the benefits of selective absorber surfaces when they may become available in the future (cf. Section 2.1.) and are generally costlier. External receivers allow for an easier scale-up to higher power levels. In particular, cylindrical designs offer a flexible design of surround heliostat fields. However, in contrast to cavity receivers, the maximum concentration of the heliostat field that could be exploited is limited by the material constraints of the heat absorbing elements, because they are located directly in the focal point.

A second criterion for the receiver design is the selected heat transfer fluid. Liquids like molten salt, liquid sodium or water/steam use irradiated tubular designs similar to those in conventional boilers, whereas for gaseous media also so-called "volumetric" absorbers are applied. They consist of high temperature resistant irradiated porous structures like wire meshes or ceramic foams. The radiation is absorbed by the material in the volume of the structure. Gas is driven through the porous material and is heated convectively. The high inner surface combined with the very small structures lead to a very efficient heat input into the gas, allowing us to transfer very high concentrated heat fluxes (0.5 MW m^{-2} to 2.5 MW m^{-2}) in spite of the poor heat conductivity of the gas. The high concentration heat fluxes lead to high receiver efficiencies (cf. Section 2.2.)

even at high gas temperatures. Temperatures of more than 1000 °C could be demonstrated in prototype receivers at the Plataforma Solar in Almería (PSA). The pros and cons of the use of the different heat transfer media are discussed subsequently.

Water/steam offers the benefit that it can be directly used in a steam-turbine cycle without further heat exchange. The evaporation of water also offers excellent heat transfer characteristics so that from that point of view water/steam receivers could be easily applied under high solar concentration. However, challenges to deal with are inhomogeneities of the heat input onto a highly pressurized absorber tube when it is irradiated only from one side and their influences on the material stability. Difficult to handle are also the start-up and transient operation of the system, leading to local changes of the cooling conditions in the absorber tubes that could result in overheating situations, in particular in the superheating section of the receiver. Finally, there is no simple solution to store large amounts of high temperature / high pressure steam, in order to operate the plant during non-sunshine hours.

Molten nitrate salts are relatively low-cost fluids that combine the benefits of being an excellent heat transfer and a perfect high temperature energy storage fluid. Depending on the specific composition it liquefies at a temperature between 120 °C and 240 °C and can be used in conjunction with metal tubes for temperatures up to 600 °C without imposing severe corrosion problems. The challenge however is to avoid freezing of the salt in any of the valves and piping of the receiver-, storage- and steam generation circuits at any time. Otherwise, extended outage periods are needed to eliminate the solid salt block impacting the profitability of the system drastically.

Air offers the benefit of being non-toxic, having no practical temperature constraints and being available for free. However, it is a poor heat transfer medium, due to its low density and low heat conductivity. The concept of volumetric receivers (see above), have paved a way how to use air for temperature levels at which molten salt or steam can not be applied. Furthermore volumetric air receivers have a very low thermal inertia allowing for rapid start-ups and dynamic response characteristics. In so called open volumetric receivers, ambient air is sucked through the porous structure and heated up to 900 °C to be used in chemical applications or to generate steam in a gas-to-water steam generator. In a pressurized variant the porous structure is placed into a pressure cavity vessel closed with a quartz glass window. At pressures of up to 15 bar and temperatures up to 1100 °C the receiver could be used to drive a gas-turbine or combined cycle system.

Power Cycle

CRSs are in most cases designed to provide a water steam cycle with heat. Compared to parabolic trough applications, today reaching an upper steam temperature below 375 °C, CRSs can be designed to provide temperatures most suitable for steam cycle power plants. For conventional power plant systems below 100 MW_e the typical steam temperature is below 550 °C and its pressure below 150 bar. Due to the excellent heat transfer characteristics molten nitrate salt systems need to be heated up to a temperature only a few K above the desired steam temperature whereas atmospheric air systems require 700 °C air temperature in order to achieve the mentioned steam conditions. Due

to a lot of difficulties concerning the control and stability of water steam receivers for this temperature range, today, saturated steam receivers with temperatures below 300 °C are the preferred option to gain commercial experience before steam superheating is addressed again.

Pressurized air receivers aim at driving a gas turbine system at a temperature level of more than 1000 °C and at a pressure between 5 bar and 15 bar. The feasibility of this concept was proven with a prototype installation at the power level of some 100 kW. The scale-up of such concepts to gas turbine systems with a higher power output would benefit from a combined cycle design (cf. Section 2.3.).

Storage

Thermal storage systems can be either based on direct storage concepts, where the heat transfer fluid is also used as the storage fluid, or on indirect storage concepts, where the heat is transferred from the heat transfer fluid to the storage medium, which can be either liquid or solid.

Nitrate molten salts are favorable fluids for a direct storage concept. In the 10 MW demonstration plant Solar Two operated between 1997 and 1999 in Barstow, California, a two tank storage concept with 100 MWh storage capacity was presented. Fluid from the cold storage tank at a temperature level of 220 °C was heated in the receiver to 570 °C and then piped into a hot storage container. Independent of the charging process, discharging was possible by using hot salt to drive a steam generator and return it to the cold tank. Future concepts may operate with a single tank with a stratified temperature distribution.

Direct **water/steam** storage concepts require large pressure vessels where saturated water steam can be stored. However, due to the high pressure required by steam turbine cycles, the container walls have to be very thick, leading to very high storage costs. Indirect storage systems premise specific temperature characteristics of the storage materials to avoid high heat transfer losses, because water evaporates or condensates at a constant temperature. One option which is under development is to use phase change materials like salt-mixtures that store the latent heat of the water – being released during the change of the water's state of aggregation – in form of the phase change energy from solid to liquid in the desired temperature range.

Air requires indirect storage concepts using solids as the storage media. To achieve a good heat transfer and to limit the pressure loss packed beds of specifically shaped high temperature resistant filling materials are utilized. A simple option is the usage of aluminum oxide spheres. Depending on the application a special container has to be designed to withstand the gas pressure.

Historical Experience and Commercial deployment

Although the number of projects of CRSs has been large, only few have culminated in the construction of entire experimental systems. In Table 2 systems that have been tested all over the world, are listed. In general terms, as it can be observed, they can be

characterized as small demonstration systems, between 0.5 MW and 10 MW, and most of them were operated in the 1980s. The thermal fluids used in the receiver were liquid sodium, saturated or superheated steam, nitrate-based molten salts and air.

Project	**Country**	**Power [MW_e]**	**Heat Transfer Fluid**	**Storage Media**	**Beginning of Operation**
SSPS	Spain	0.5	Liquid Sodium	Sodium	1981
EURELIOS	Italy	1	Steam	Nitrate Salt / Water	1981
SUNSHINE	Japan	1	Steam	Nitrate Salt / Water	1981
Solar One	U.S.A.	10	Steam	Oil / Rock	1982
CESA - 1	Spain	1	Steam	Nitrate Salt	1982
MSEE / Cat B	U.S.A.	1	Nitrate Salt	Nitrate Salt	1983
THEMIS	France	2.5	Hitec Salt	Hitec Salt	1984
SPP - 5	Russia	5	Steam	Water / Steam	1986
TSA	Spain	1	Air	Ceramic	1993
Solar Two	U.S.A.	10	Nitrate Salt	Nitrate Salt	1996
Consolar	Israel	0.5 [a]	Pressurized Air	Fossil Hybrid	2001
Solgate	Spain	0.3	Pressurized Air	Fossil Hybrid	2002
PS 10	Spain	10	Saturated Steam	Steam Drum	2006
[a] Thermal					

Table 2: Central Receiver System Projects (cf. Romero et al., 2002)

The set of referred experiences has served a demonstration of the technical feasibility of the CRS power plants, whose technology is sufficiently mature. The most extended experience has been collected by several European projects located in Spain at the premises of the Plataforma Solar de Almería and in the USA with the 10-MW Solar One and Solar Two plants that can be seen in Figure 23.

Figure 23: The Solar Two CRS in Barstow (California, U.S.A.)
(Courtesy of Sandia National Laboratories)

Annual efficiencies of 7 % have been demonstrated; the predictions are that efficiencies of 23 % at design point and 20 % annual will be reached by 2030 with investment costs of 0.9 \$ W_p^{-1}. Three of the most promising power tower technologies that are expected to lead to commercial plants are described in this chapter:

- molten salt technology,
- open or closed loop volumetric air technologies and
- saturated steam technology.

For each of the three concepts the first commercial deployment is in preparation. In 2006 a molten salt system named Solar Tres with a power level of 15 MW is being developed in Spain. A saturated steam system of 10 MW capacity is under construction close to Seville (Spain), a 1.5 MW atmospheric air receiver system will be set up in Germany and a 300 kW pressurized air system is under construction in Sicily (Italy). Those systems intend to be a first generation of commercial demonstration plants, which has to be built to validate the technology under real operation and market conditions before larger scale deployment can be started.

Performance Cascade

Figure 24 shows the waterfall diagram of the annual performance of the experimental 10 MW water steam CRS Solar One and the extrapolation to an optimized 100 MW commercial system. Losses under "Utilized irradiation" include outages, start-up and shut-down periods as well as radiation levels that are too low for electric power production. "Reflected from collector field" includes losses by imperfect reflections,

cosine losses, atmospheric attenuation from the heliostat to the tower and shading of the heliostats. "Incident on receiver" accounts for radiation that missed the receiver. "Thermal from receiver" accounts for reflections and heat losses form the receiver. "Thermal to storage" means piping heat losses, "Thermal to turbine" accounts for heat losses from the storage. "Gross electric" reflects the annual thermal efficiency of the power cycle. In "Net electric" parasitic power requirements to run pumps and motors are considered. The real Solar One figures have demonstrated an annual efficiency of only 5.7 %. However, based on the experience with this demonstration plant a larger and optimized system may reach about 16 % annual efficiency. Experience gathered in upcoming demonstration projects will hopefully provide a broader data basis of performance figures for solar power plants.

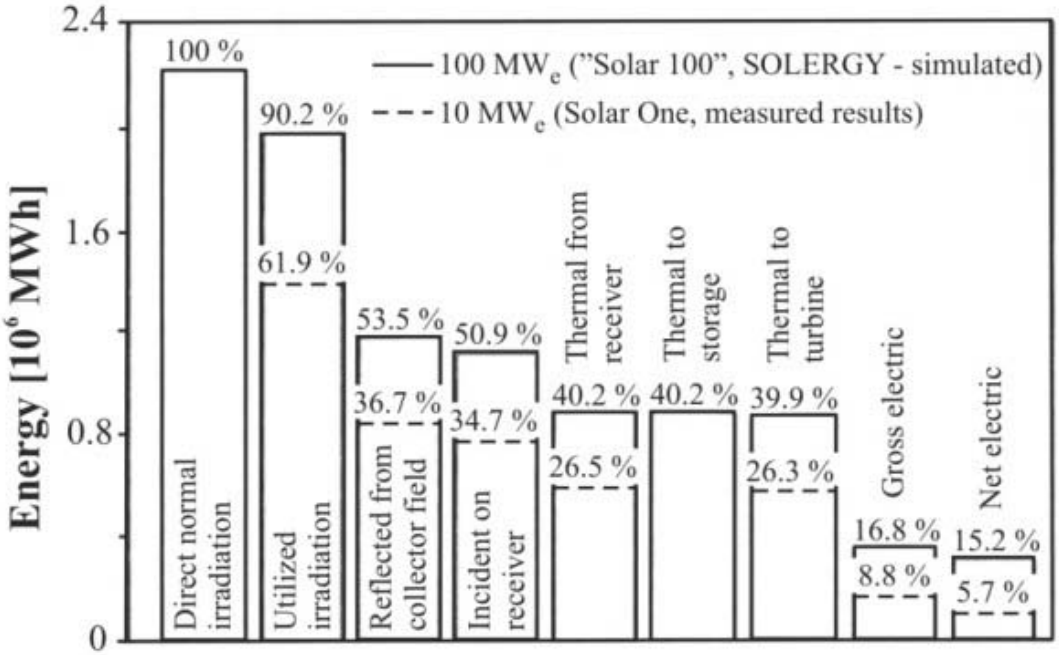

Figure 24: Annual Performance of a central receiver system, measured and simulated (Based on Grasse, 1988. With kind permission of the publisher.)

3.3. Solar Furnaces

A solar furnace is the third concept of high temperature solar concentrating systems and is discussed in this chapter. Other than the two concepts described above, a solar furnace is generally not designed to produce electricity via high temperature heat, but is utilized as a research tool to apply very high energy densities to materials or processes under investigation. In this tool, the flexibility and the accessibility of the focus point is of higher importance than the cost of concentration. The product of value coming out of a solar furnace is primarily knowledge and not energy.

A solar furnace consists of a primary solar collection system (usually a varying number of flat faceted heliostats). It redirects the solar radiation onto a static parabolic concentrator which concentrates the incoming radiation onto a fixed spot. Since the geometrical arrangement of incoming and outgoing rays of the concentrator does not

change over time a solar furnace achieves almost constant optical properties independent of the sun's position. It provides a fixed focus position, so that even heavy experimental equipment could be easily put in place. One or two attenuators can be arranged in the optical path to control the power of the solar furnace according to the needs of the respective experiments or to provide quickly fluctuating radiation pulses, e.g. for thermal shock experiments. The experiment is generally mounted on a test table which is moveable in three dimensions to adjust it to the focal point.

The basic characteristic that makes solar furnaces attractive is the possibility of applying very high energy densities to a material almost instantly and, if necessary, under controlled atmospheres, avoiding undesirable poisonous processes. Depending on the size and the concentration properties of the furnace, the focal spot has a diameter in the order of magnitude of a few to several 10 cm, which is considerably larger than the relevant area of those treatments using lasers, arc lamps, electron beams, etc. Furthermore, solar furnace experiments can be performed in oxygenating atmospheres, whereas most conventional high temperature furnaces need vacuum conditions to protect the heating elements. However, there are also disadvantages to be considered: The intermittence of the solar energy input (day/night, clouds) as well as its change in intensity lead to limited periods of constant operation conditions. Additionally, the radiation input is not uniform in space but can typically be represented by a three-dimensional Gaussian profile. Moreover, the number of potential useful testing hours depends significantly on the site conditions. Finally the overall cost of such an installation is relatively high.

Two optical arrangements can be distinguished in solar furnaces. In the classical layout the relative position of the concentrating elements with regard to the collector is a north/south-alignment with the focal point being located on the axis between both. This is called *on-axis* position. Some facilities, which have been built recently, however, use the *off-axis* concept, in which, there is not such an alignment (see Figure 25). The advantage of this system is that the work area does not shade the concentrator and the focal spot can be easily provided inside of a building. Special mention should be made of a furnace with a vertical optical axis, the 6.5 kW solar furnace at Odeillo (France), which uses light reflected vertically by heliostats (see Figure 26: indicated as MSSFs). Its orientation enables tests of pieces in the horizontal plane, which is very advantageous, when treatments involve melting materials.

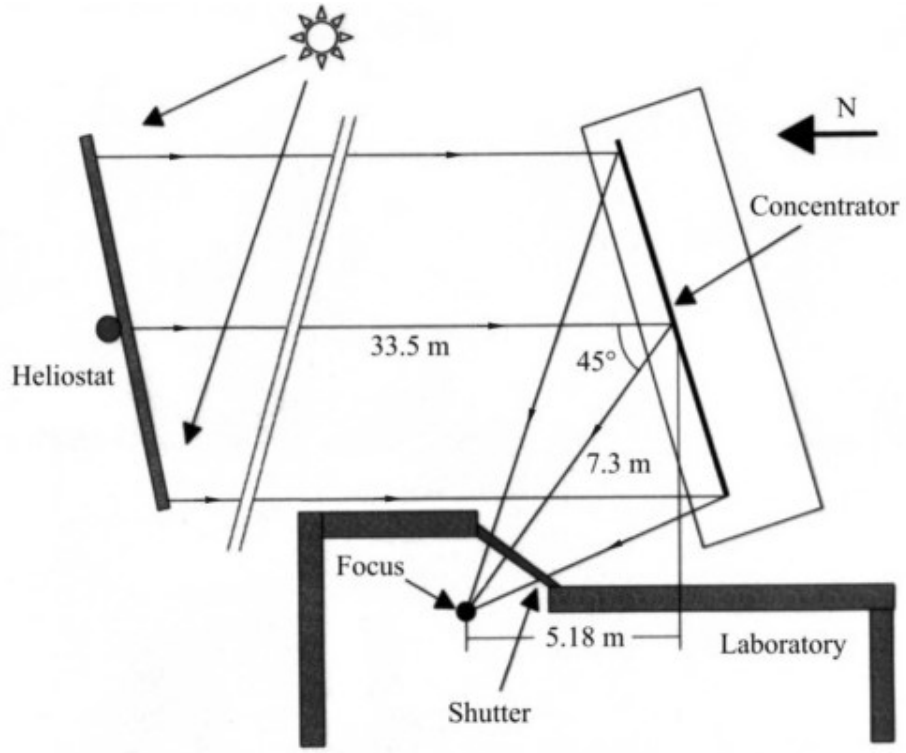

Figure 25: Scheme of the off-axis solar furnace in Cologne (Germany) (Source: DLR)

Historical overview

Applied research in solar furnaces started at the beginning of the 1950s. Perhaps, the greatest motivation for the use of this peculiar source of thermal energy was the study of the effects of the "new" nuclear weapons on all types of materials and the search for possible candidates for protection. The time profile (Nuclear Thermal Transient) of a nuclear explosion can be easily reproduced in a Solar Furnace. Military solar furnaces were built in White Sands (New Mexico, U.S.A.), and in the French 'Laboratoire Central de l'Armament' in the Eastern Pyrenees.

In the beginning work was strictly basic research with wide publications of refractory material phase diagrams ($A1_2O_3$, ZrO_2 etc.), studies on ignition, kinetic studies on refractory materials, crystal growth for use in semiconductors, solar cells and lasers.

Another field of study has been the field of thermophysical properties of materials at high temperatures, such as mechanical properties, spectral emissivity, thermal expansion, thermal conductivity, absorption and diffusion as well as electrical properties.

In all these activities, a common difficulty, innate to the energy source, has appeared in the inability to find out the exact temperature on the irradiated surface. Sensors, vulnerable to the incident radiation density, cannot be placed on the exposed surface, since even if they could withstand the concentrated radiation, they would measure their own temperature instead of that of the sample.

This has given rise to research into the entirely new field of non-contact temperature measurement (pyrometry) and into new measurement systems determining the flux densities in the focal plane.

With the development of different concentrated solar energy applications, solar furnaces have slightly modified the direction of their activities. The follow-up of the solar chemistry of the 1970s, mainly in the hands of French researchers, and the appearance of the volumetric receiver concept in power generating CRS inspired the use of furnaces for the small-scale pre-testing before their full-size implementation.

At the end of the 1980s and the beginning of the 1990s several new furnaces were installed. Chronologically, these are:

- 1989: Solar furnace at the Paul Scherrer Institute (PSI) (Switzerland)
- 1989: Solar furnace at the National Renewable Energies Laboratory (NREL) (U.S.A.)
- 1991: Solar furnace at the Plataforma Solar de Almería (PSA) (Spain)
- 1994: Solar furnace at the German Aerospace Center (DLR) (Germany)

Lamp concentrators in the typical solar furnace arrangement but using a set of Xe-lamps instead of the sun as the radiation source were set up at the PSI in 2005 and are under construction in the DLR.

Three typical designs of solar furnaces are presented below.

1. A scheme of the arrangement of the 1000 kW solar furnace in Odeillo (France) and with similar in Taskent (Uzbek) can be seen in Figure 26. The furnace in Odeillo was inaugurated in 1970 and consists of a field of 63 heliostats on eight terraces each with a surface of 45 m² as a collector. The concentrator is integrated into the building and has a dimension of 40 m height and 54 m width. Because of its large half angle of the radiation cone coming from the concentrator concentration factors of close to 10 000 can be achieved (see Figure 27).

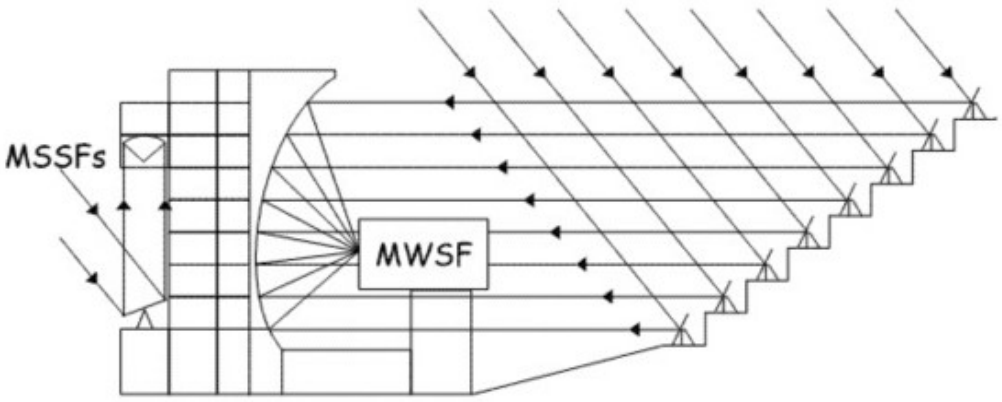

Figure 26: Scheme of the solar furnaces in Odeillo (France) (Source: PROMES-CNRS) (MWSF: Mega Watt Solar Furnace, MSSFs: Medium Size Solar Furnaces)

Figure 27: The 1000 kW solar furnace in Odeillo (France) (Source: PROMES-CNRS)

2. Smaller on-axis furnaces with a similar design but using a single heliostat are located in Israel at the Weizmann Institute of Science (WIS), at the Sandia National Laboratories (SNL) in Albuquerque (U.S.A.) and at the PSI (see Figure 28) in Switzerland. They reach a power level between 16 kW and 40 kW and concentration ratios between 5000 and 10 000 (PSI) without secondary optics.

Figure 28: Small on-axis solar furnace at the PSI (Source: PSI)

The 60 kW furnace at the PSA uses one 120 m² flat faceted heliostat (see Figure 29). This application achieves a concentration ratio of 4000.

Figure 29: The 60 kW solar furnace at the PSA (Source: PSA)

3. Solar furnaces of 15 kW to 20 kW in off-axis configurations are available in Golden (Colorado, U.S.A.) and Cologne (Germany) (see Figure 30) with concentration factors of about 5000. Both facilities use the concentrated beam inside of a laboratory building.

Figure 30: Solar furnace in Cologne (Source: DLR)

4. Conclusions

Today high temperature solar concentrators are used as one option for solar electricity production, e.g. as dish/Stirling or central receiver system. As solar furnaces they

represent a research tool to apply very high energy densities to materials or processes under investigation. After a long period of gaining practical experiences with pilot plants and research facilities, the systems have started to enter the commercial market in recent years – mainly in the field of electricity production. Cost reduction for solar thermal electricity generation is strongly linked to an increased system performance which goes hand in hand with increased operation temperatures. In addition, the use of high temperature heat becomes increasingly attractive for renewable fuel production like the thermochemical water splitting producing hydrogen. These concepts require temperatures significantly higher than the temperatures needed for the electricity generation. This fact results in new challenges for R&D activities in the field of high temperature solar concentrators.

Acknowledgments

The author gratefully acknowledges the kind permission of Springer Science and Business Media and VDI-Verlag to use desired materials. He thanks PROMES-CNRS (Laboratoire Procédés, Matériaux et Energie Solaire - Centre National de la Recherche Scientifique), PSA (Plataforma Solar de Almería), PSI (Paul Scherrer Institute), SNL (Sandia National Laboratories), SES (Stirling Energy Systems) and SOLO Stirling for the provision of meaningful figures. The editorial support of Michael Wullenkord is highly acknowledged.

Glossary

Absorber:	Object that transfers radiation power into heat.
AM (Air Mass):	Factor which describes the distance through the atmosphere that radiation has to pass. AM equals one for perpendicular irradiation conditions.
Aperture:	Opening of an optical system.
Black body:	Item that is an ideal absorber of electromagnetic radiation. Neither transmittance nor reflection occurs.
Cosine loss:	Loss mechanism based on the non perpendicular orientation of radiation related to a surface. The radiation power is distributed over a larger area compared to perpendicular conditions and thus the energy density is reduced.
Fresnel concentrator:	Concentrator that consists of numerous elements each one with a special shape forming a part of a paraboloid and mounted in a common plane.
On-axis:	Configuration of a concentrating system where the focus spot is part of the axis between the collector and the concentrator. In contrast there is not such an alignment in off-axis systems.
Parabolic trough:	Two dimensional concentrator with a parabolic shape forming a trough. The absorber is a tube that is mounted in the focus line.
Receiver:	Item that includes the absorber. Cavity and external designs are used.

Nomenclature

A	m^2	Entrance aperture area
A'	m^2	Exit aperture area
A_{Ab}	m^2	Absorber area
A_{Ap}	m^2	Aperture area
C	-	Concentration factor
C_{max}	-	Maximum concentration factor (46 200)
c	$m\ s^{-1}$	Velocity of light in vacuum ($2.99792458 \cdot 10^8$)
D	m	Lens diameter
E	$W\ m^{-2}$	Energy density
E^S	$W\ m^{-2}$	Radiation density of the direct solar radiation
$E^{S/}$	$W\ m^{-2}$	Density of incoming solar radiation (after concentration)
E'	$W\ m^{-2}$	Energy density (outgoing)
E_λ	$Wm^{-2}\mu m^{-1}$	Spectral energy density of the radiation
F	-	Heat removal factor
f	m	Focal length
f	-	Dilution factor
h	$W\ s^2$	Planck constant ($6.6260755 \cdot 10^{-34}$)
h_1	$kJ\ kg^{-1}$	Specific enthalpy (condition 1)
h_2	$kJ\ kg^{-1}$	Specific enthalpy (condition 2)
k	$W\ s\ K^{-1}$	Boltzmann constant ($1.380658 \cdot 10^{-23}$)
Q	W	Useful heat
Q_{in}	W	Heat input
s	$kJkg^{-1}K^{-1}$	Specific entropy
s_1	$kJkg^{-1}K^{-1}$	Specific entropy (condition 1)
s_2	$kJkg^{-1}K^{-1}$	Specific entropy (condition 2)

T	K	Temperature
T_A	K	Temperature of the absorber
T_a	K	Temperature of the ambiance
T_F	K	Average temperature of the heat transfer fluid
T_H	K	Upper temperature of the Carnot cycle
T_m	K	Average temperature
T_0	K	Lower temperature
U_I	W m^{-2}	Inner heat transfer coefficient (from absorber to fluid)
U_L	W m^{-2}	Heat loss coefficient (convection and conduction)
W	W	Work
α	-	Absorptivity
ε	-	Emissivity
η_C	-	Carnot-efficiency
η_{th}	-	Efficiency of the receiver
η_{tot}	-	Total system efficiency (solar receiver and heat conversion)
λ	µm	Wavelength
λ_C	µm	Cut-off wavelength
Φ	W	Radiation energy
σ	Wm$^{-2\ -4}$	Stefan-Boltzmann constant ($5.67051 \cdot 10^{-8}$)
Θ	mrad	Half angle of a radiation cone (incoming)
Θ'	mrad	Half angle of a radiation cone (outgoing)

Bibliography

Grasse W. (1988). Entwurfsgrundlagen für solarthermische Kraftwerke – Ergebnisse und Erfahrungen aus demBetrieb von Experimentalanlagen. In: VDI-Gesellsch. Energietechnik (Ed.). *VDI-Berichte 704 Solarthermische Kraftwerke zur Wärme- und Stromerzeugung*. Düsseldorf, Germany: VDI-Verlag. (page 184, figure 7)[Report about the operation of pilot solar power plants (e. g. Solar One).]

Mancini T., Heller P. (Eds.) (2003). Dish-Stirling Systems: An Overview of Development and Status. *Journal of Solar Energy Engineering* **125**, 135-151.[Review of different dish/Stirling systems including technical and economical details.]

Mancini T. (Ed.) (2000). SolarPACES Technical Report No. III – 1/00. Catalog of Solar Heliostats, 32 pp.[This catalog comprehends an overview about heliostats purchasable in 2000 with detailed information.]

Plataforma Solar de Almería (Ed.) (2004). *Annual Report 2004*, 102 pp. Tabernas, Spain. (page 20, figure 17)[Presentation of PSA with detailed information about the facilities, infrastructures and R&D projects in 2004.]

Romero M., Buck R., Pacheco J.E. (2002). An Update on Solar Central Receiver Systems, Projects and Technologies. *Journal of Solar Energy Engineering* **124**, 98-108.[Review of different Solar Central Receiver projects and plans.]

Sizmann R., with contributions by Köpke P. and Busen R. (1991). Solar Radiation Conversion. In: Winter C.-J., Sizmann R.L., Vant Hull L.L. (Eds.). *Solar Power Plants. Fundamentals, Technology, Systems, Economics*. Berlin, Germany: Springer. (page 50, figure 2.24)[Textbook about solar power plants: this chapter provides information about solar radiation, its conversion to heat or electricity, and its use in photochemical processes.]

Stine W.B., Harrigan R.W. (1985). *Solar Energy Fundamentals and design*, 536 pp. New York: Wiley & Sons.[Textbook about Solar Energy.]

Welford W.T., Winston R. (1978). *The Optics of Nonimaging Concentrators. Light and Solar Energy*, 200pp.San Diego, CA, USA: Academic Press.[Book about non-imaging concentrators (e. g. compound parabolic concentrators) implying basic geometrical optics and applications.]

Winter C.-J., Sizmann R.L., Vant Hull L.L. (Eds.) (1991). *Solar Power Plants. Fundamentals, Technology,Systems, Economics*, 424 pp. Berlin, Germany: Springer.[Comprehensive textbook about solar power plants.]

Biographical Sketch

Prof. Dr.-Ing. Robert Pitz-Paal is head of the Solar Research Unit at the German Aerospace Center (DLR) and Professor for Solar Technology at the Technical University in Aachen. He has been working in the field of concentrating solar systems for more than 15 years. He has served as the Operating Agent for Task III of the SolarPACES (Solar Power and Chemical Energy Systems) implementing agreement of the International Energy Agency and is its Vice Chairman today. He is also member of the editorial board of the ASME Journal of Solar Energy Engineering. His team has been awarded the title “Center of Excellence” in the field of Concentrating Solar Technology by DLR Board of Directors in 2006.

To cite this chapter
Robert Pitz-Paal, (2007) , HIGH TEMPERATURE SOLAR CONCENTRATORS, in *Solar Energy Conversion and Photoenergy Systems* , [Ed. Julian Blanco Galvez, Sixto Malato Rodriguez], in *Encyclopedia of Life Support Systems (EOLSS),* Developed under the Auspices of the UNESCO, Eolss Publishers, Oxford ,UK, [http://www.eolss.net]